12. SITE 724[1]

Shipboard Scientific Party[2]

HOLE 724A

Date occupied: 20 September 1987

Date departed: 20 September 1987

Time on hole: 16 hr

Position: 18°27.713′N, 57°47.147′E

Water depth (sea level; corrected m, echo-sounding): 592.8

Water depth (rig floor; corrected m, echo-sounding): 603.3

Bottom felt (m, drill pipe): 602.5

Penetration (m): 44.5

Number of cores: 5

Total length of cored section (m): 44.5

Total core recovered (m): 44.8

Core recovery (%): 100.7

Oldest sediment cored:
Depth sub-bottom (m): 44.8
Nature: foraminifer nannofossil ooze
Age: Pleistocene
Measured velocity (km/s): 1.6

HOLE 724B

Date occupied: 20 September 1987

Date departed: 21 September 1987

Time on hole: 15 hr

Position: 18°27.713′N, 57°47.147′E

Water depth (sea level; corrected m, echo-sounding): 592.8

Water depth (rig floor; corrected m, echo-sounding): 603.3

Bottom felt (m, drill pipe): 602.0

Penetration (m): 257.7

Number of cores: 27

Total length of cored section (m): 257.7

Total core recovered (m): 213.7

Core recovery (%): 82.9

Oldest sediment cored:
Depth sub-bottom (m): 257.7
Nature: calcareous clayey silt
Age: early Pliocene
Measured velocity (km/s): —

HOLE 724C

Date occupied: 21 September 1987

Date departed: 21 September 1987

Time on hole: 16 hr

Position: 18°27.713′N, 57°47.147′E

Water depth (sea level; corrected m, echo-sounding): 592.8

Water depth (rig floor; corrected m, echo-sounding): 603.3

Bottom felt (m, drill pipe): 603.2

Penetration (m): 252.4

Number of cores: 27

Total length of cored section (m): 252.4

Total core recovered (m): 242.7

Core recovery (%): 96.2

Oldest sediment cored:
Depth sub-bottom (m): 252.4
Nature: calcareous clayey silt
Age: early Pliocene
Measured velocity (km/s): —

Principal results: Site 724 is at a water depth of about 600 m in the northern part of the upper slope basin on the continental margin of Oman. It is the central drilling target of a depth transect that corresponds to the vertical extent of a pronounced mid-water oxygen-minimum zone.

The major findings at Site 724 include identification of the following:

1. Laminated facies of late Pliocene age that are similar to, but older than, the organic-carbon- and opal-rich facies found at Site 723.
2. An interval of abundant preservation of radiolarians and diatoms and concomitant poor preservation of planktonic foraminifers that occurs near the Pliocene/Pleistocene boundary and is partially coincident with the laminated facies.
3. The occurrence of shallow-water benthic foraminifers in the upper Pliocene section, which may indicate substantial subsidence of the site over the past 3 to 4 m.y.
4. An ongoing reduction of sulfate over the entire section and low Mg^{2+} concentrations. In contrast to Site 723, diagenetic dolomites were not encountered.
5. Trace amounts of ethane, propane, and butane increase steadily with depth.

Overall, Site 724 provides new information about the subsidence of slope basins between basement ridges and on the history of the carbon-rich, opal-rich laminated facies that are associated with the oxygen-minimum zone along the continental margin.

BACKGROUND AND OBJECTIVES

Site 724 of the Ocean Drilling Program (ODP) is in a water depth of about 593 m at 18°27.713′N, 57°47.147′E, on the continental margin of Oman. The site position is near the center of the upper slope basin that was previously drilled at Site 723. The location of Site 724 is shown in Figures 1 and 2, and the structural and depositional setting of the site is shown in Figure 3. At this location, the slope basin is only about 5 km wide, compared to 15 km at Site 723. It is bounded on the west by a faulted block and on the east by a basement ridge. Both basement features are thought to be ophiolite complexes.

Seismic-reflection profiles of the basin sediments show numerous highly reflective layers that both onlap onto and are de-

[1] Prell, W. L., Niitsuma, N., et al., 1989. *Proc. ODP, Init. Repts.*, 117: College Station, TX (Ocean Drilling Program).

[2] Shipboard Scientific Party is as given in the list of Participants preceding the contents.

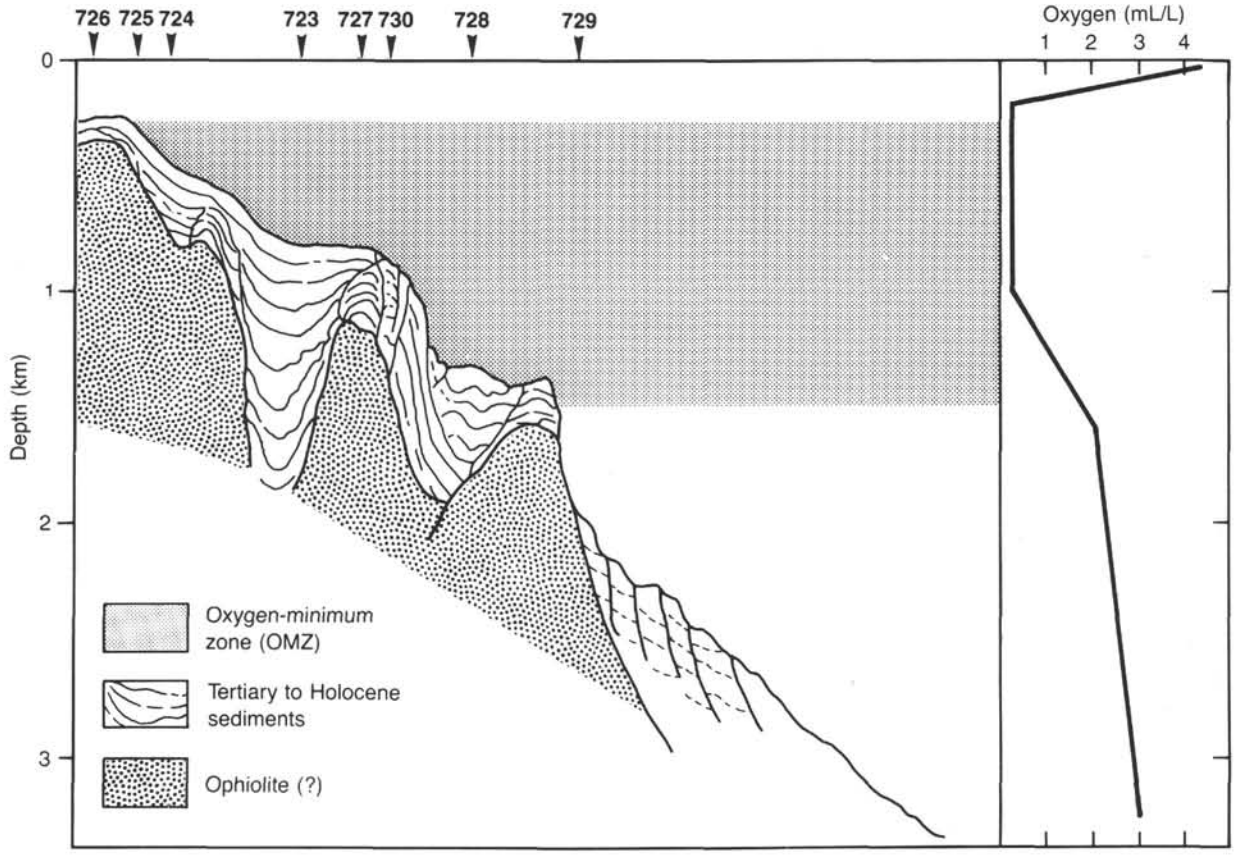

Figure 1. Structure of the Oman margin and the oxygen-minimum zone. The schematic cross section across the margin shows the series of basement ophiolite blocks and the sedimentary basins between them. The concentration of oxygen in the water column (RC2704; unpubl. data, 1986) defines the depth range of the oxygen-minimum zone and where it impinges on the margin.

formed by the adjacent basement structures. The sediments are thickest in the center of the basin and form a syncline-shaped deposit (Fig. 3A) that thickens significantly to the south along the strike of the basin (Fig. 3B). In the shallow sediments near Site 724, some channeling is observed about 5 km to the north, and a large slump scar is noted about 9 km to the south (Fig. 3B). The east-west slope of the sediment surface from the shelf to the seaward edge of the basin is about 2%. The subsurface layers (reflectors) shoal slightly over the basement high, from which they deepen to the south. Comparison of reflector depths at Sites 723 and 724 indicates that the average accumulation rates at Site 724 should be about one-half those at Site 723. Site 724 was located in a water depth of about 600 m to provide samples from the middle of the oxygen-minimum zone in an area with an estimated accumulation rate of about 80 m/m.y. Thus, the site was expected to provide an additional high-resolution sedimentary record of Pliocene-Pleistocene variations of monsoonal upwelling and the oxygen-minimum zone.

The specific objectives for drilling at Site 724 were:

1. To obtain a high-resolution record of the sediments associated with the near-coastal zone of the monsoonal upwelling system, in order to establish the changes in timing and intensity of the monsoon.
2. To provide part of a depth transect that will be used to examine the organic-rich sedimentary facies of the margin and establish their relationship to the oxygen-minimum zone and its spatial variation through time.
3. To document the diagenetic processes associated with the oxygen-minimum zone and the organic-carbon-rich sediments.
4. To search for evidence of changes in the structure of the intermediate water masses of Arabian Sea during the Pliocene-Pleistocene.

OPERATIONS

JOIDES Resolution departed Site 723 at 0030 hr on 20 September 1987. A combined seismic survey of drilling targets OM-3 (Site 724) and OM-4 (Site 725) was begun upon departure. The ship's track during the survey is shown in Figure 4.

After locating the site on the survey line, the beacon was lowered on a taut wireline in 592.8 m water depth at 1045 hr. The position of Site 724 was assessed as 18°27.713′N and 57°47.147′E by the global positioning satellite system.

The mud line of Hole 724A was shot at 1200 hr on 20 September (Table 1). After successfully coring to Core 117-724A-5H with the advanced piston corer (APC) system (0.0 to 44.5 m below seafloor [mbsf] at 100.7% recovery), the core barrel parted during retrieval of Core 117-724A-6H at an overpull of 120,000 lb, and Hole 724A had to be abandoned.

Hole 724B was spudded at 1600 hr on 20 September without offsetting the rig, and five APC cores, averaging 102% recovery, were obtained from the interval 0.0 to 45.0 mbsf before switching to the extended core barrel (XCB) system. Coring of Hole 724B ended at total depth of 257.7 mbsf, the target depth, after cutting Core 117-724B-27X. Average recovery for the 22 XCB cores was 79%. As was the case at Site 723, core expansion caused by gas was severe throughout the cored section. Overall recovery in Hole 724B was 82.9% (Table 1).

After clearing the mudline of Hole 724B at 0800 hr on 21 September, Hole 724C was spudded after offsetting 10 m to the

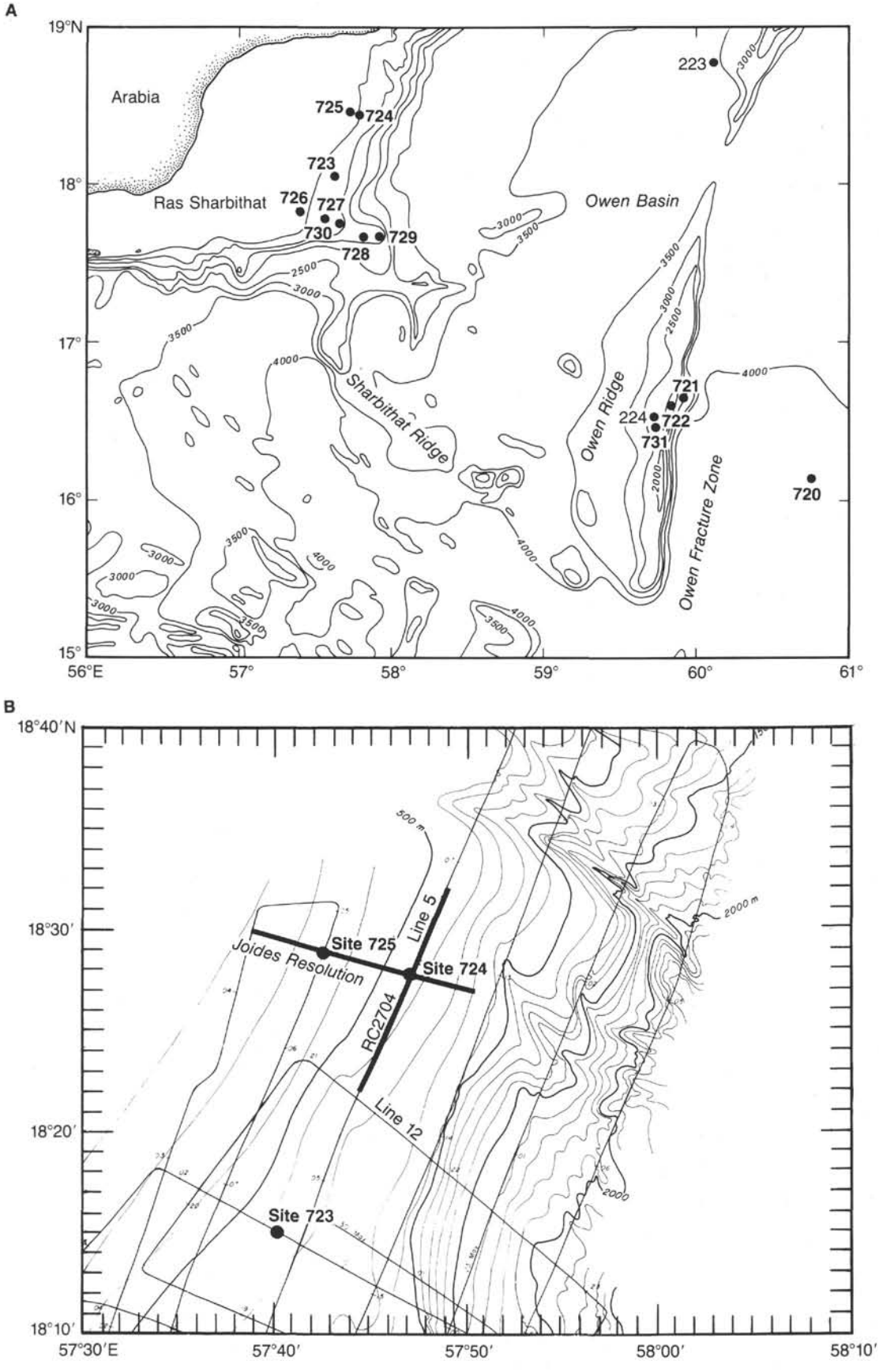

Figure 2. **A.** Bathymetry of the Oman margin (in meters) and the location of Site 724. **B.** Detailed location of Site 724 and the seismic profiles shown in Figure 3. Bathymetry (in meters) and seismic data are from the site survey (RC2704; unpubl. data, 1986).

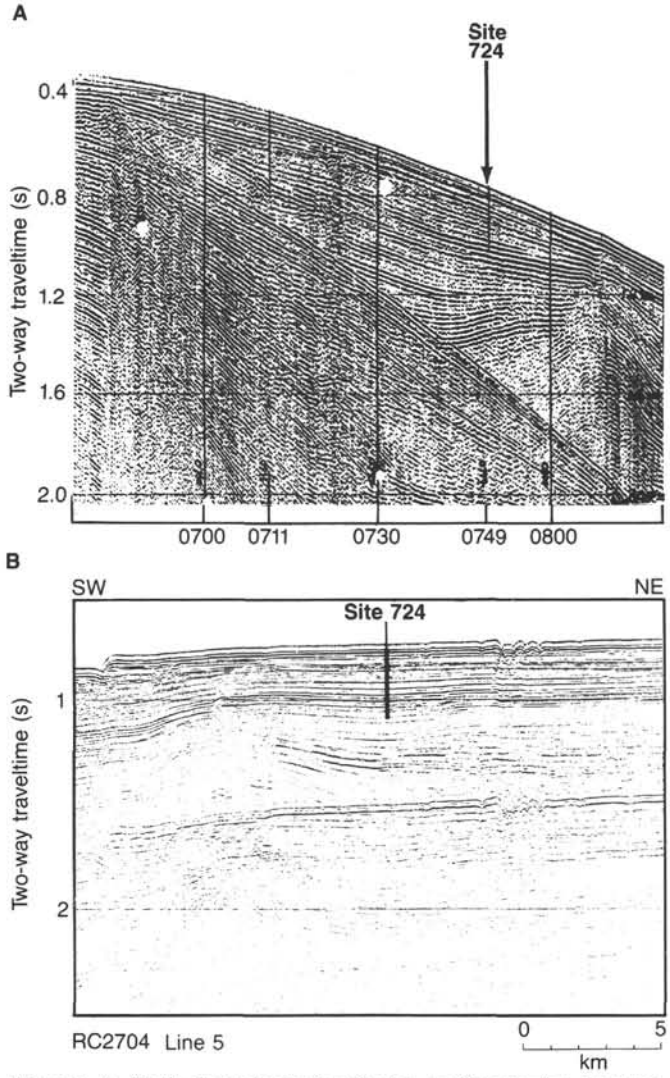

Figure 3. **A.** Single-channel seismic-reflection profiles showing the structural and depositional setting of Site 724. *JOIDES Resolution* line is perpendicular to the trend of the basin and shows the bounding basement blocks and the syncline-shaped sediment fill. **B.** RC2704 Line 5 is positioned along the strike of the basin and shows the sediment thickness decreasing to the northeast.

southwest at 0830 hr. Recovery of five APC cores (0.0 to 40.8 mbsf) averaged 105%, whereas coring in XCB mode for the remaining cores to 252.4 mbsf total depth averaged 94%, including voids from core expansion. Average recovery for the 27 cores was 96.2%. The hole was displaced with weighted mud, the pipe was pulled, and the ship was underway in dynamic positioning mode to relocate to Site 725 by 2400 hr on 21 September.

LITHOSTRATIGRAPHY

Lithologic Units

Unit I (Depth, 0–257.7 mbsf; Age, Holocene–early Pliocene)

Cores 117-724A-1H through 117-724A-5H, 117-724B-1H through 117-724B-27X, and 117-724C-1H through 117-724C-27X.

Only one lithologic unit is recognized at Site 724. Unit I is subdivided into two facies, as indicated on Figure 5. The calcareous clayey silt facies (facies I) comprises the entire sedimentary sequence of Hole 724A and the majority of Holes 724B and 724C. A laminated diatomaceous clayey silt facies (facies II) forms beds a few decimeters to meters thick in the lower cores of Holes 724B and 724C (Table 2).

Facies I: Calcareous Clayey Silt

Facies I dominates the sedimentary sequence at Site 724 and consists of black (5Y 2.5/2), very dark gray (5Y 3/1), olive gray (5Y 4/2, 5/2), and olive (5Y 5/3) beds. The beds range from 5 cm to about 250 cm thick, with most beds between 50 and 200 cm. Contacts are predominantly burrow mottled and gradational over a few centimeters, although some contacts are extremely sharp.

Based on smear slide data (areal percentages illustrated in Fig. 6) the average composition of this facies is approximately 30% clay, 25% detrital calcite, 10% quartz (mainly silt size), 20% nannofossils, and 2% foraminifers. The smear slides also contain trace amounts of glauconite, collophane, dolomite, and organic matter. A few horizons contain over 30% nannofossils (55% maximum) and have lower detrital calcite, clay, and quartz contents (Fig. 6). Quartz and clay contents remain fairly constant throughout this facies. Foraminifers increase from an average of 5% in Cores 117-724A-1H, 117-724B-1H, and 117-724C-1H to about 15% in Cores 117-724B-11X and 117-724C-11X. Foraminifers decrease in Cores 117-724B-14X and 117-724C-14X, and from there on, values remain near 2% down to Cores 117-724B-18X and 117-724C-18X. Below the development of facies II in Cores 117-724B-19X to 117-724B-23X and 117-724C-19X to 117-724C-23X, the foraminifer content returns to around 10%.

According to the geochemical data (Figs. 7 and 8 and Table 3), facies I has an average carbonate content of 55% above Cores 117-724B-19X and 117-724C-19X; below Cores 117-724B-23X and 117-724C-23X, the average carbonate content is 47%. In general, the carbonate values from smear slides (nannofossils, foraminifers, and detrital calcite) agree with the geochemical values for particular stratigraphic levels to within 15%, although the former is based on areal percent rather than weight percent. The total organic carbon (TOC) determinations (Table 3) average 1.4% for facies I. Smear slide data show that the light (olive, 5Y 4/3, and olive gray, 5Y 5/2) beds of the calcareous clayey silt facies tend to have more nannofossils and less clay than the dark (black, 5Y 2.5/2, very dark gray, 5Y 3/1, dark olive gray, 5Y 3/2, and olive gray, 5Y 4/2) beds. An unusual development of facies I is a 1- to 1.5-m-thick layer of finely bedded calcareous clayey silt that lacks burrow mottles. (The term "finely bedded" is used here merely to distinguish this layer in facies I from the "laminated" beds of facies II.) The finely bedded layer occurs in all three holes at Site 724 at about 16 mbsf and consists of millimeter- to centimeter-scale beds, averaging about 5 mm in thickness, which are alternately dark olive gray (5Y 3/2) and olive gray (5Y 4/2). Identical sediments were observed at 25 mbsf at Site 723.

Phosphatic or apatite nodules occur at several horizons at Site 724 (Fig. 5). Two types of nodules were observed: a soft yellow brown (10YR 5/6) variety with an elliptical cross section of a mean diameter ranging from 5 to 20 mm and a hard black to dark gray variety with an irregularly shaped cross section of a mean diameter ranging from 2 to 50 mm. The second variety commonly has surface impressions of what may have been woody material (now decomposed). The phosphatic composition of these nodules was demonstrated by X-ray diffraction (XRD) and a test involving crystals of ammonium molybdate and dilute nitric acid, which turn yellow in the presence of phosphorus (G. Shimmield, pers. comm., 1987). One of the hard nodules is illustrated in Figure 9 with its XRD trace shown in Figure 10.

Facies II: Laminated Diatomaceous Clayey Silt

This facies forms beds from 5 to 175 cm thick (average 62 cm) with laminae less than 1 mm thick. The laminae are dark olive gray (5Y 3/2), olive gray (5Y 4/2), and olive (5Y 5/4). Smear slide results from seven laminae yield a mean composi-

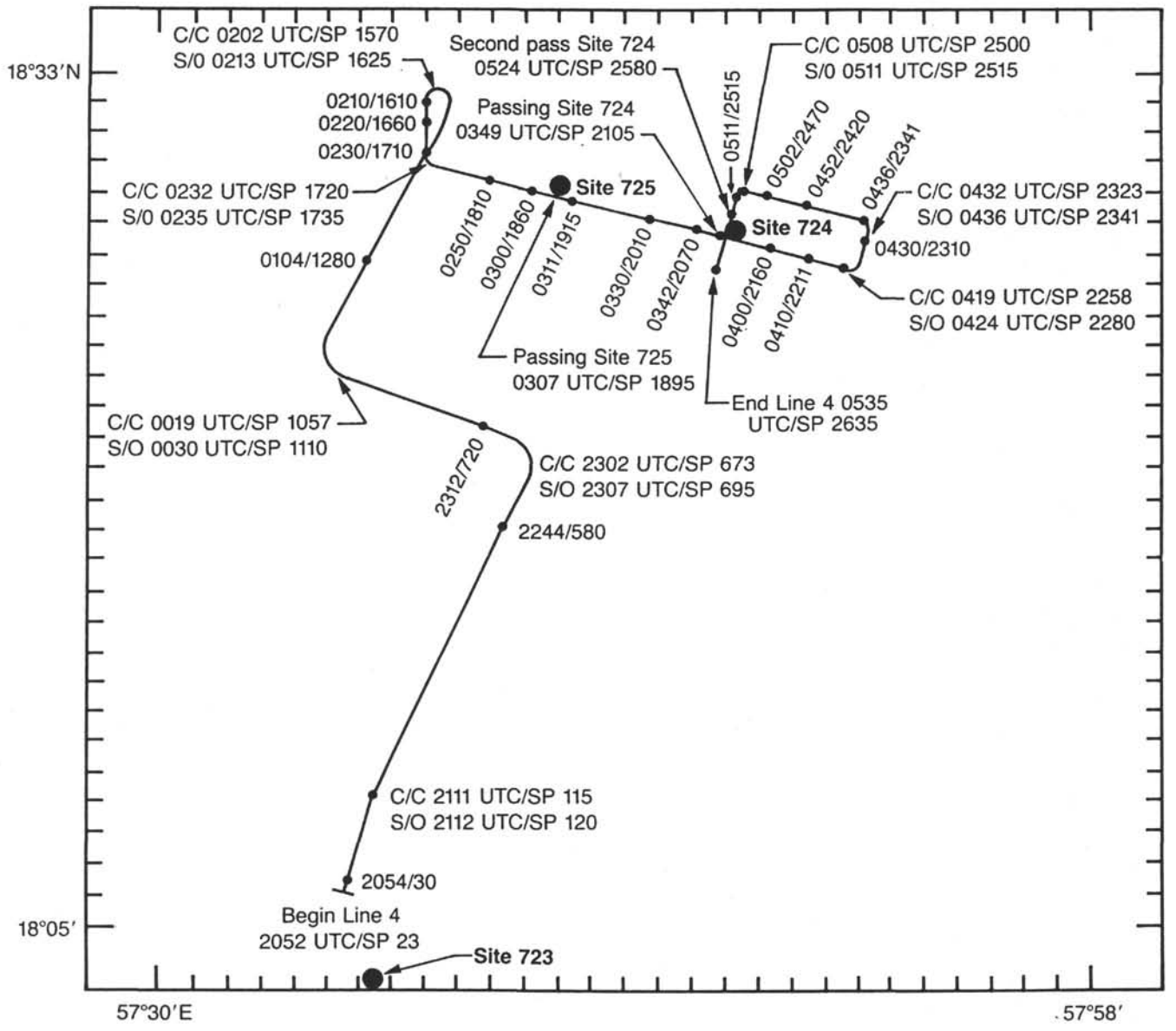

Figure 4. Ship's track during survey of Sites 724 and 725 and positioning at Site 724.

tion of 46% diatoms (60% maximum), 33% clay, 7% detrital calcite, 6% quartz, and 2% nannofossils. Highly similar sediments were found at Sites 723, 725, and 726. Geochemical determinations show that carbonate and organic carbon contents are extremely variable in Cores 117-724B-19X to 117-724B-23X and 117-724C-19X to 117-724C-23X. In these cores both facies I and II are present, which accounts for some of this variability. Average values in this interval are 8% carbonate and 5.5% TOC.

Discussion

The diatomaceous and laminated sediment of facies II appears to indicate a depositional environment that differed intermittently from that represented by the bioturbated calcareous clayey silt of facies I. The preservation of lamination indicates a lack of bioturbation, which implies that the bottom waters were anoxic. The high TOC values in facies II might partly reflect the lack of oxygen in the bottom waters. It is not known if the postulated low oxygen contents were a consequence of high primary productivity in the surface waters and/or the result of a stratified water column through which organic matter fell. The high silica content of facies II might indicate a high production of siliceous organisms. Alternatively, silica might have been largely dissolved in the bioturbated, calcareous sediments, but preserved in the less calcareous, unbioturbated, and laminated sediments. Whatever mechanism is invoked to explain the laminated sediment, late Pliocene conditions were different than in the Pleistocene, because none of the Oman margin sites (723 to 730) recovered laminated sediment in the upper Pleistocene to Holocene section.

Of particular interest at this site is the zone of low foraminifer concentration in Cores 117-724B-15X to 117-724B-23X and 117-724C-15X to 117-724C-23X (Fig. 6). This zone is not restricted to the occurrence of diatomaceous laminated sediment (facies II). The benthic foraminifers apparently remain at nearly constant concentration throughout Cores 117-724B-15X to 117-724B-23X and 117-724C-15X to 117-724C-23X. On the other hand, coccoliths are poorly preserved, planktonic foraminifers are reduced in numbers, and those species that are least resistant to dissolution are missing in this zone (see "Biostratigraphy" section, this chapter). The average carbonate content of facies I

Table 1. Coring summary for Site 724.

Core no.	Date (Sept. 1987)	Time	Depth (mbsf)	Cored (m)	Recovered (m)	Recovery (%)
117-724A-						
1H	20	1240	0.0–6.5	6.5	6.50	100.0
2H	20	1300	6.5–15.9	9.4	9.20	97.9
3H	20	1315	15.9–25.4	9.5	9.65	101.0
4H	20	1330	25.4–34.9	9.5	9.54	100.0
5H	20	1345	34.9–44.5	9.6	9.87	103.0
				44.5	44.76	
117-724B-						
1H	20	1615	0.0–7.0	7.0	7.05	101.0
2H	20	1630	7.0–16.4	9.4	9.75	104.0
3H	20	1650	16.4–25.9	9.5	9.71	102.0
4H	20	1705	25.9–35.4	9.5	9.70	102.0
5H	20	1730	35.4–45.0	9.6	9.97	104.0
6X	20	1810	45.0–54.7	9.7	7.10	73.2
7X	20	1840	54.7–64.4	9.7	5.95	61.3
8X	20	1910	64.4–74.0	9.6	7.18	74.8
9X	20	1935	74.0–83.7	9.7	8.56	88.2
10X	20	2005	83.7–93.4	9.7	3.81	39.3
11X	20	2035	93.4–103.0	9.6	7.59	79.0
12X	20	2055	103.0–112.7	9.7	9.88	102.0
13X	20	2120	112.7–122.4	9.7	0.00	0.0
14X	20	2135	122.4–132.0	9.6	10.04	104.6
15X	20	2200	132.0–141.7	9.7	2.67	27.5
16X	20	2225	141.7–151.4	9.7	10.09	104.0
17X	20	2250	151.4–161.0	9.6	9.97	104.0
18X	20	2315	161.0–170.7	9.7	9.94	102.0
19X	20	2350	170.7–180.4	9.7	9.89	102.0
20X	21	0025	180.4–190.0	9.6	9.45	98.4
21X	21	0110	190.0–199.7	9.7	4.85	50.0
22X	21	0145	199.7–209.4	9.7	1.24	12.8
23X	21	0220	209.4–219.0	9.6	9.74	101.0
24X	21	0250	219.0–228.7	9.7	9.70	100.0
25X	21	0315	228.7–238.4	9.7	9.83	101.0
26X	21	0340	238.4–248.0	9.6	10.06	104.8
27X	21	0425	248.0–257.7	9.7	9.23	95.1
				257.7	212.95	
117-724C-						
1H	21	0830	0.0–2.8	2.8	2.82	101.0
2H	21	0855	2.8–12.2	9.4	9.93	105.0
3H	21	0915	12.2–21.7	9.5	10.05	105.8
4H	21	0935	21.7–31.2	9.5	10.14	106.7
5H	21	1000	31.2–40.8	9.6	9.88	103.0
6X	21	1055	40.8–50.5	9.7	8.94	92.1
7X	21	1120	50.5–60.2	9.7	8.78	90.5
8X	21	1140	60.2–69.8	9.6	8.52	88.8
9X	21	1205	69.8–79.4	9.6	9.57	99.7
10X	21	1225	79.4–89.0	9.6	7.76	80.8
11X	21	1250	89.0–98.6	9.6	9.75	101.0
12X	21	1315	98.6–108.3	9.7	9.82	101.0
13X	21	1345	108.3–117.8	9.5	10.04	105.7
14X	21	1410	117.8–127.4	9.6	8.41	87.6
15X	21	1440	127.4–137.0	9.6	10.12	105.4
16X	21	1505	137.0–146.6	9.6	10.35	107.8
17X	21	1530	146.6–156.3	9.7	9.73	100.0
18X	21	1610	156.3–165.9	9.6	9.33	97.2
19X	21	1655	165.9–175.5	9.6	3.41	35.5
20X	21	1725	175.5–185.2	9.7	9.09	93.7
21X	21	1800	185.2–194.8	9.6	5.86	61.0
22X	21	1840	194.8–204.5	9.7	10.61	109.4
23X	21	1910	204.5–214.1	9.6	10.50	109.4
24X	21	1945	214.1–223.7	9.6	9.69	101.0
25X	21	2015	223.7–233.4	9.7	9.09	93.7
26X	21	2035	233.4–242.9	9.5	10.08	106.1
27X	21	2100	242.9–252.4	9.5	10.43	109.8
				252.4	242.70	

in Cores 117-724B-19X to 117-724B-23X and 117-724C-19X to 117-724C-23X is only 36%, which may provide supporting geochemical evidence for a zone of carbonate dissolution. The zone of low foraminifer concentration seems to indicate a period of carbonate dissolution in the late Pliocene to early Pleistocene. It is primarily associated with the occurrence of the laminated sediment (facies II), indicating that the dissolution may be connected to the conditions that led to anoxic bottom waters.

In comparison with Site 723, the sediments deposited at Site 724 contain a greater proportion of terrigenous material (clay, quartz, and detrital calcite). The proportion of terrigenous material might have been determined by the relative water depth and the proximity of the coastline.

Sites 723 and 724 can be correlated lithologically using the finely bedded layer of facies I (Cores 117-724A-2H and 117-724B-2H through 117-723B-4H). The origin of this layer and the significance of the correlation are not yet clear. The laminated diatomaceous beds occur near the Pliocene/Pleistocene boundary at both sites (Table 2). A preliminary comparison of the thicknesses and relative positions of these beds revealed a similarity in the distribution of groups of laminated beds at the Pliocene/Pleistocene boundary and in the upper Pliocene.

A prominent sedimentary feature of Site 723 is a series of dolomitized beds and stringers (see "Lithostratigraphy" section, "Site 723" chapter, this volume). The topmost dolomite layer at Site 723 was recovered from the lowermost Pleistocene. Although Pliocene sediments were recovered at Site 724, no dolomite was encountered. This probably reflects a difference in the diagenetic history of the two sites, because Site 724 lacks a substantial subsurface supply of sulfate and magnesium ions from below (see "Inorganic Chemistry" section, this chapter). Phosphorite and apatite nodules were found at Site 724 but not at Site 723 even though both sites have relatively high values of TOC (one requirement for the formation of phosphorite). However, both sites show major differences in sedimentation rates during the Pliocene and Pleistocene (80 m/m.y. at Site 724, 175 m/m.y. at Site 723). Phosphorite nodules grow slowly, close to the sediment/water interface, which requires slow sedimentation rates for formation. Therefore, the presence of phosphorite at Site 724 and its absence at Site 723 were controlled in part by the sedimentation rates (see "Inorganic Chemistry" section). However, the sedimentation rate at Site 724 is higher than would normally be associated with phosphorite formation, and possibly, the formation of phosphorite was linked to winnowing that left no trace other than the nodules themselves.

BIOSTRATIGRAPHY

Site 724 is on the seaward flank of an upper slope basin. The upper Neogene sediments of this relatively shallow (593 m water depth) site, which is currently within the oxygen-minimum zone, were deposited at a high rate and were expected to record changes in sedimentation resulting from oceanographic and atmospheric circulation.

Planktonic and benthic foraminifers, nannofossils, and radiolarians in the sediments cored at Site 724 were analyzed to obtain biostratigraphic datum levels and to record the faunal changes caused by coastal upwelling. The Pliocene/Pleistocene boundary was recognized at about 130 mbsf (Fig. 11). A plot of faunal datum levels and paleomagnetic reversals vs. depth below seafloor is presented in Figure 12; Table 4 is a detailed listing of these data points.

Throughout the upper part of Hole 724B (0–161.0 mbsf), planktonic and benthic foraminifers and calcareous nannofossils are abundant and moderately to well preserved. Foraminifers exhibit high species diversity, whereas the nannofossils have comparatively low species diversity.

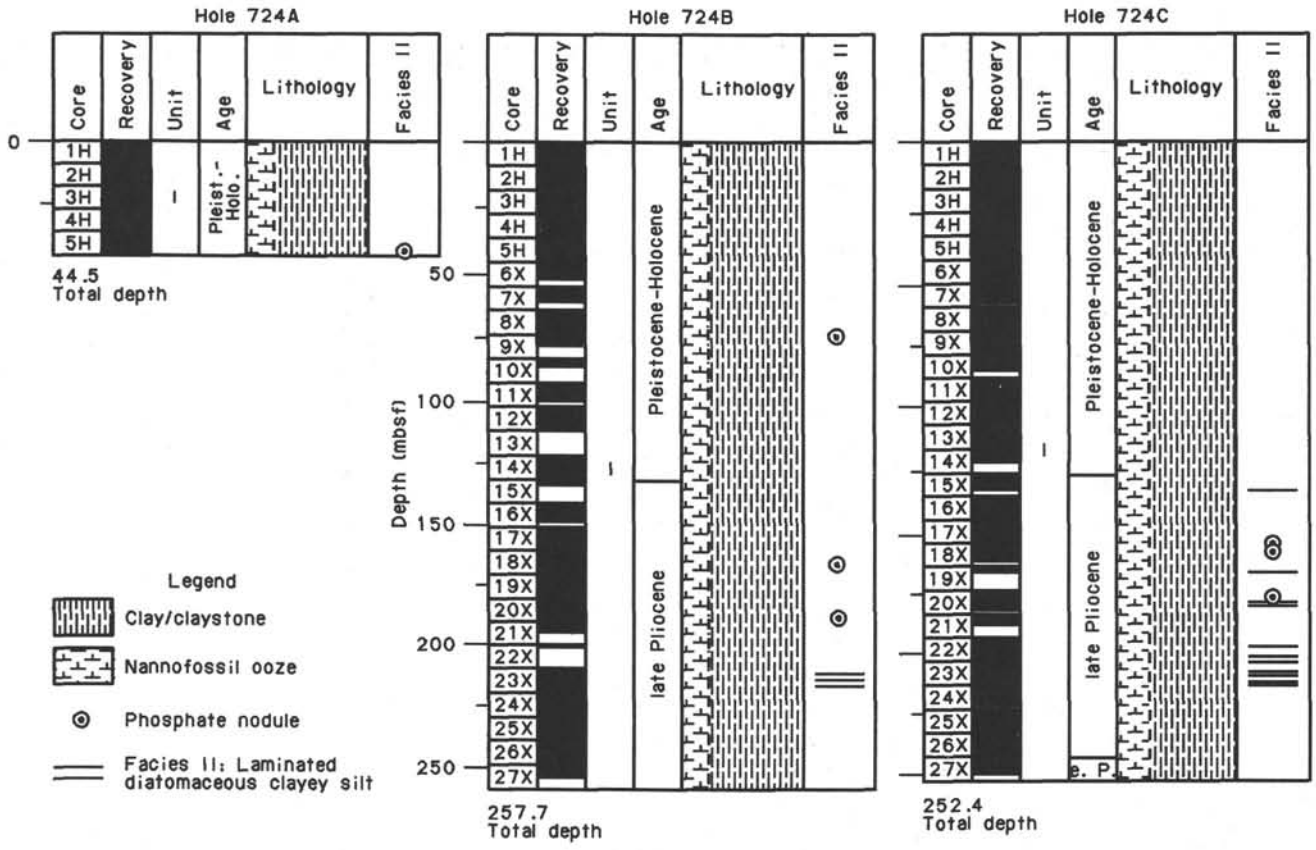

Figure 5. Lithologic summary column for Holes 724A, 724B, and 724C.

Table 2. Stratigraphic occurrence of facies II (laminated diatomaceous clayey silt) at Site 724.

Core, section, interval (cm)	Depth (mbsf)
117-724B-	
23X-5, 62–120	216.02–216.60
23X-6, 118–150	218.08–218.40
23X-7, 0–37	218.40–218.77
23X, CC (0–21)	218.79–219.00
117-724C-	
15X-4, 80–85	132.70–132.75
19X-1, 35–45	166.25–166.35
20X-4, 24–82	180.24–180.82
22X-2, 123–150	197.53–197.80
22X-5, 100–140	201.80–202.20
22X-6, 102–119	203.32–203.49
22X, CC (22–41)	204.31–204.50
23X-1, 106–150	
23X-2, 0–150	205.56–207.58
23X-3, 0–8	
23X-3, 148–150	208.98–210.35
23X-4, 0–135	

Below approximately 161.0 mbsf, the preservation of the calcareous nannofossils becomes poor, and planktonic foraminifers and nannofossils decrease in abundance. At about 225 mbsf this trend reverses: nannofossils and planktonic foraminifers increase in abundance and their preservation improves to a moderate level. These conditions persist to the bottom of the hole. The investigation of calcareous nannofossils in Hole 724C corroborates this general pattern.

The distribution and preservation of siliceous microfossils has an inverse relationship to that of the calcareous nannofossils. Radiolarians and diatoms are absent or present in low amounts to 190 mbsf. From 190 to 229 mbsf, radiolarians become more abundant but the species diversity is low. From 248 mbsf to the bottom of the hole, the radiolarian abundance decreases.

The presence of shallow-water benthic foraminifers in the lower part of the sequence is probably indicative of a subsiding seafloor since the latest early Pliocene.

Planktonic Foraminifers

The distribution of planktonic foraminifers in Hole 724B is similar to that observed in Hole 723A. Highly diverse faunas are found in the upper part of the sequence (Samples 117-724B-1H, CC through 117-724B-16X, CC; 7.0–151 mbsf), where they are abundant and their preservation is good. Pleistocene Zones N23 and N22 are recognized for this part of the section, which consists of foraminifer-bearing nannofossil oozes. The zonal boundary was noted between Samples 117-724B-9X, CC and 117-724B-10X, CC (83.8–93.4 mbsf), as *Globigerinella calida calida* is present in the former but not in the latter sample.

Downhole, foraminifers are rare and moderately well- to poorly preserved (Samples 117-724B-17X, CC through 117-724B-25X, CC; 161.0–238.4 mbsf). Samples 117-724B-26X, CC and 117-724B-27X, CC (248.0–257.7 mbsf) contain common planktonic foraminifers with moderate preservation.

The position of the Pleistocene/Pliocene boundary is difficult to determine because *Globorotalia truncatulinoides* and *Globorotalia tosaensis* are missing at this boundary. An obvious late Pliocene age assemblage is present in Sample 117-724B-19X, CC (180.4 mbsf), because common *Globorotalia acostaensis* and *Globorotalia humerosa* and some *Globorotalia limbata* specimens are found. The absence of the zonal marker of Zone

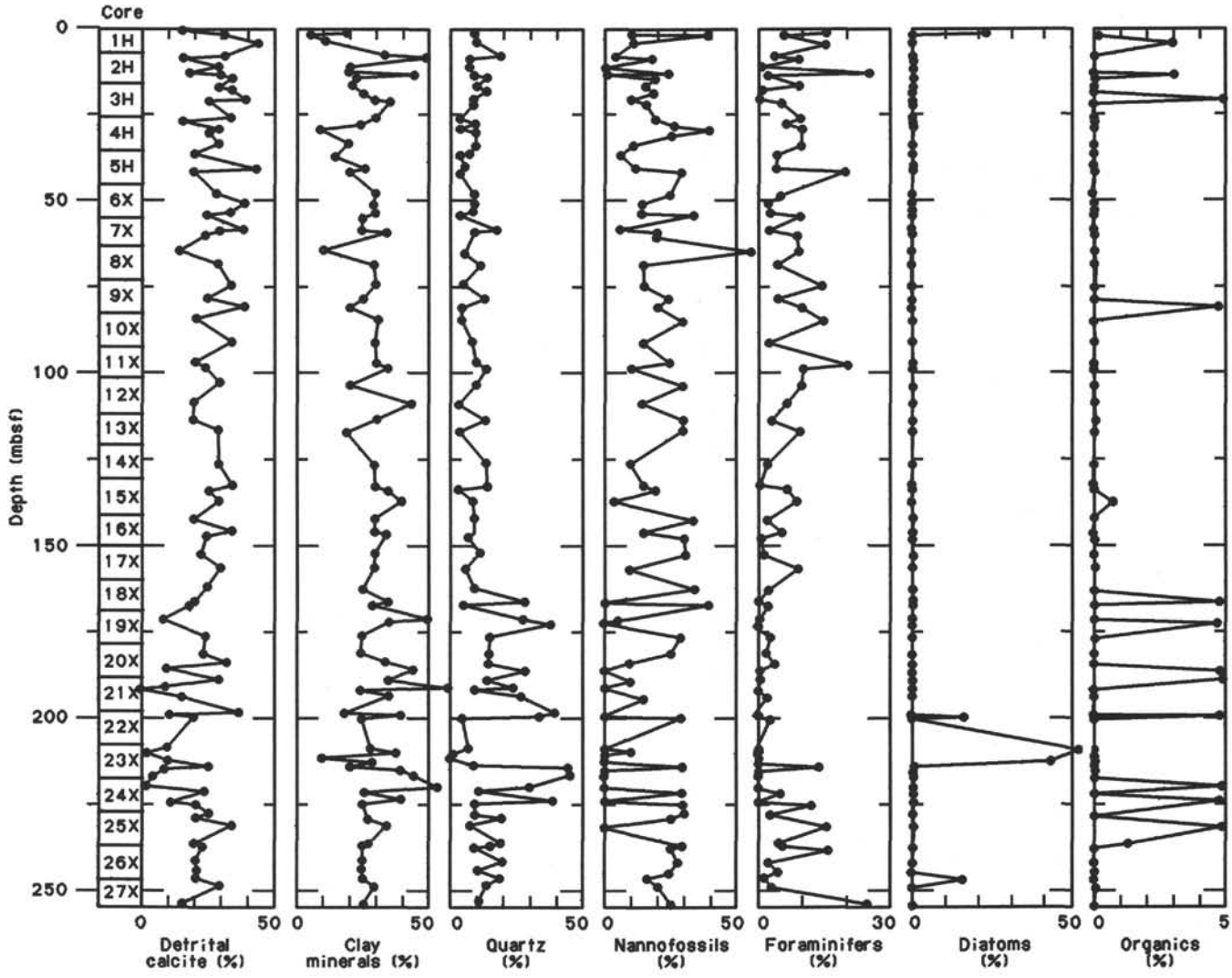

Figure 6. Smear slide data for Holes 724A, 724B, and 724C.

N21 prevented its discrimination from Zone N19–20 in the Pliocene. However, the presence of common *Turborotalia nigriniae* specimens in Samples 117-724B-26X, CC and 117-724B-27X, CC (248.0–257.7 mbsf) shows that the basal part of Hole 724B can be assigned to Zones N19 to N20 and is early to middle Pliocene in age (Fleisher, 1974).

Benthic Foraminifers

The benthic foraminiferal fauna was studied in the core-catcher samples of Hole 724B. The benthic fauna is characterized by its numerous species and high abundance. The state of preservation is moderate to good.

The benthic foraminiferal fauna is dominated by *Bolivina ordinaria*, which comprises between 20% and 70% of the fauna in the samples studied. Other benthic species occurring in high relative abundance throughout the sequence are *Hyalinea baltica* and *Uvigerina peregrina*. Less abundant, but present in most samples, are *Bulimina marginata, Bulimina mexicana, Epistominella* cf. *exigua, Florilus* sp. A, *Stilostomella* spp., and *Uvigerina auberiana*. The foraminiferal fauna is rather uniform in most of the samples, and there are no significant changes in the sequence studied, with the exception of the presence of *Ammonia beccarii* in the lowermost four samples (Samples 117-724B-24X, CC, through 117-724B-27X, CC; 228.7–257.7 mbsf).

According to van Morkhoven et al. (1986), the stratigraphic range for *H. baltica* is upper Pliocene (N21) through Pleistocene (N23). At this site, however, the presence of *H. baltica* throughout the sequence studied places the first occurrence of this species in lower Pliocene (N19) or lower.

Significant in most samples are numerous minor gastropods, pelecypods, and scaphopods. Phosphoritized fish teeth and vertebrae are present throughout the studied sequence.

Calcareous Nannofossils

Three holes were drilled at Site 724 (Fig. 13). Calcareous nannofossils are abundant throughout Hole 724A (6.5–44.5 mbsf), and the preservation is moderate to good. Nannofossils in Hole 724B are abundant with moderate preservation through Sample 117-724B-16X, CC (to 151.4 mbsf). Abundance remains high, but preservation becomes worse and stays poor through Sample 117-724B-18X, CC (151.4–170.7 mbsf). The number of nannofossils decreases to one specimen per 1–10 fields of view whereas preservation remains poor through Sample 117-724B-23X, CC (170.7–219.0 mbsf). At this depth, abundance increases again, and preservation improves to a moderate level. These conditions persist to the bottom of the hole (219.0–257.7 mbsf). Hole 724C has abundant nannofossils with moderate preservation through Sample 117-724C-18X, CC (to 165.9 mbsf). As was the case in

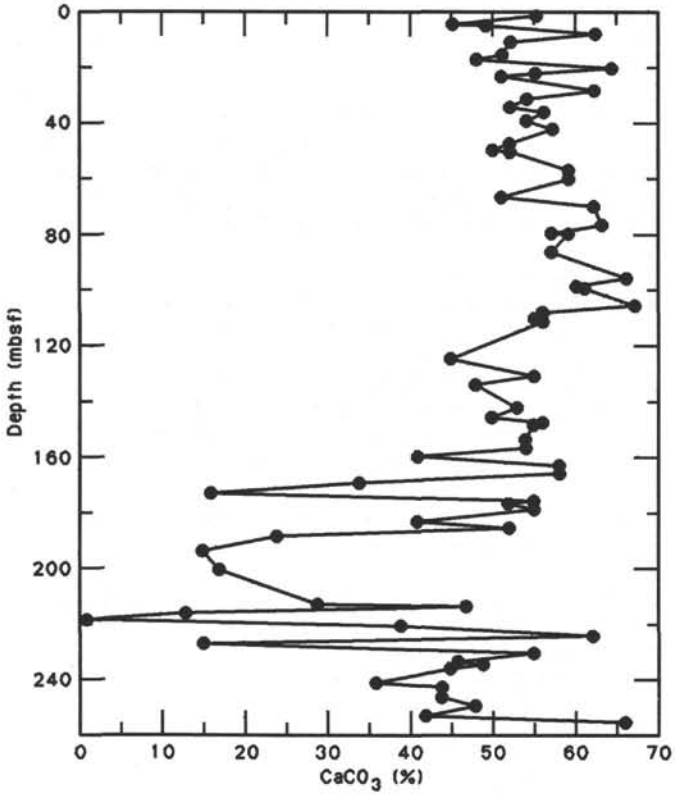

Figure 7. $CaCO_3$ profile (see Table 3) for Holes 724A and 724B.

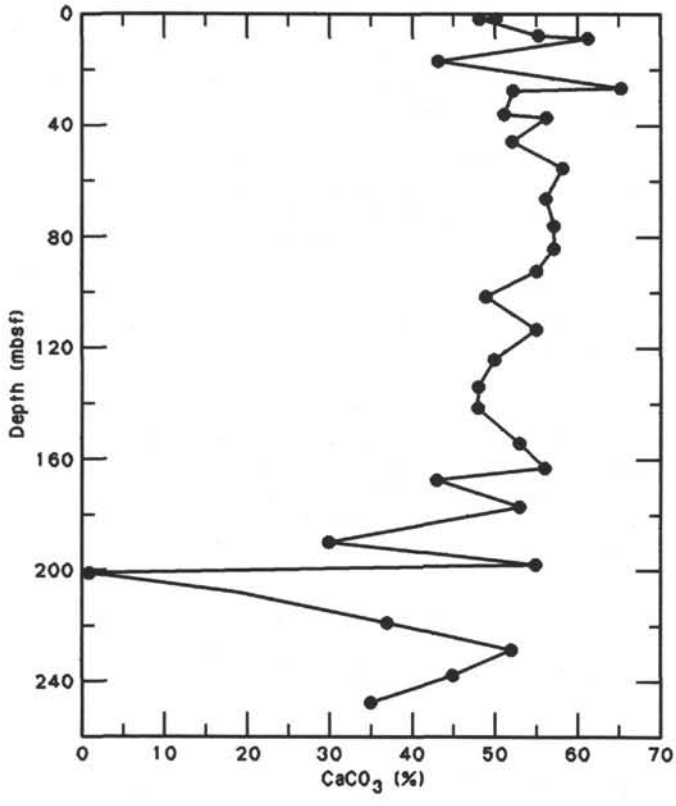

Figure 8. $CaCO_3$ profile (see Table 3) for Hole 724C.

Table 3. Organic carbon and carbonate carbon percentages.

Core, section, interval (cm)	Depth (mbsf)	Total carbon (%)	Inorganic carbon (%)	Organic carbon (%)	$CaCO_3$ (%)
724A-1H-1, 100–102	1.00		6.67		55.6
724C-1H-2, 0–1	1.50	7.16	6.11	1.05	50.9
724C-1H-2, 48–50	1.98		5.85		48.7
724A-1H-3, 100–102	4.00		5.42		45.2
724A-1H-3, 144–145	4.44	6.65	5.91	0.74	49.2
724A-2H-1, 100–102	7.50		7.49		62.4
724C-2H-4, 48–50	7.78		6.63		55.2
724C-2H-5, 0–1	8.80	8.84	7.41	1.43	61.7
724A-2H-3, 100–102	10.50		6.25		52.1
724A-2H-6, 100–102	15.00		6.14		51.2
724A-3H-1, 100–102	16.90		5.80		48.3
724C-3H-4, 48–50	17.18		5.16		43.0
724A-3H-3, 100–102	19.90		7.72		64.3
724A-3H-4, 144–145	21.84	8.01	6.60	1.41	55.0
724A-3H-5, 100–102	22.90		6.18		51.5
724C-4H-4, 48–50	26.68		7.83		65.2
724C-4H-5, 0–1	27.70	8.41	6.31	2.10	52.6
724A-4H-2, 100–102	27.90	8.83	7.50	1.33	62.5
724A-4H-4, 100–102	30.90	7.74	6.57	1.17	54.7
724A-4H-6, 100–102	33.90	6.65	6.33	0.32	52.7
724A-5H-1, 100–102	35.90	7.51	6.82	0.69	56.8
724C-5H-4, 48–50	36.18		6.14		51.2
724C-5H-5, 0–1	37.20	8.31	6.78	1.53	56.5
724A-5H-3, 100–102	38.90	8.01	6.51	1.50	54.2
724A-5H-5, 100–102	41.90	8.25	6.86	1.39	57.1
724C-6X-4, 48–50	45.78		6.28		52.3
724B-6X-2, 70–72	47.20		6.29		52.4
724B-6X-3, 144–145	49.44	6.84	6.09	0.75	50.7
724B-6X-4, 70–73	50.20		6.25		52.1
724C-7X-4, 48–50	55.48		6.97		58.1
724B-7X-2, 70–72	56.90		7.17		59.7
724B-7X-4, 70–72	59.90		7.13		59.4
724C-8X-5, 32–34	66.52		6.75		56.2
724B-8X-2, 80–82	66.70		6.23		51.9
724B-8X-4, 80–82	69.70		7.47		62.2
724C-9X-5, 50–52	76.30		6.91		57.6
724B-9X-2, 90–92	76.40		7.58		63.1
724B-9X-4, 90–92	79.40		6.88		57.3
724B-9X-4, 119–120	79.69	8.77	7.11	1.66	59.2
724C-10X-4, 34–36	84.24		6.93		57.7
724B-10X-2, 90–92	86.10		6.87		57.2
724C-11X-3, 57–59	92.57		6.61		55.1
724B-11X-2, 74–76	95.64		8.01		66.7
724B-11X-4, 74–76	98.64		7.26	60.5	
724B-11X-4, 149–150	99.39	9.30	7.32	1.98	61.0
724C-12X-3, 20–22	101.80		5.99		49.9
724B-12X-2, 98–100	105.48		8.04		67.0
724B-12X-4, 68–70	108.18		6.80		56.6
724B-12X-4, 95–97	108.45		6.72		56.0
724B-12X-5, 119–120	110.19	8.70	6.71	1.99	55.9
724B-12X-6, 88–90	111.38		6.78		56.5
724C-13X-4, 86–88	113.66		6.62		55.1
724C-14X-5, 79–81	124.59		6.00		50.0
724B-14X-2, 80–82	124.70		5.49		45.7
724B-14X-6, 90–92	130.80		6.70		55.8
724B-15X-2, 50–52	134.00		5.79		48.2
724C-15X-5, 90–92	134.30		5.83		48.6
724C-16X-4, 50–52	142.00		5.76		48.0
724B-16X-1, 71–73	142.41		6.47		53.9
724B-16X-3, 91–93	145.61		6.04		50.3
724B-16X-4, 144–145	147.64	8.97	6.78	2.19	56.5
724B-16X-5, 77–79	148.47		6.70		55.8
724B-17X-2, 85–87	153.75		6.52	54.3	
724C-17X-6, 67–69	154.77		6.38		53.2
724B-17X-4, 81–83	156.71		6.49		54.1
724B-17X-6, 105–107	159.95		4.95		41.2
724B-18X-2, 50–52	163.00		7.05		58.7
724C-18X-5, 111–113	163.41		6.75		56.2
724B-18X-4, 57–59	166.07		7.01		58.4
724C-19X-2, 66–68	168.06		5.22		43.5
724B-18X-6, 82–84	169.32		4.18	34.8	
724B-19X-2, 88–90	173.08		1.97		16.4
724B-19X-4, 74–76	175.94		6.66		55.5
724B-19X-5, 0–1	176.70	9.53	6.29	3.24	52.4
724C-20X-2, 76–78	177.76		6.43		53.6
724B-19X-6, 70–72	178.90		6.63	55.2	
724B-20X-2, 125–12	183.15		4.93		41.1

Table 3 (continued).

Core, section, interval (cm)	Depth (mbsf)	Total carbon (%)	Inorganic carbon (%)	Organic carbon (%)	$CaCO_3$ (%)
724B-20X-4, 70–72	185.60		6.25		52.1
724B-20X-6, 75–77	188.65		2.89		24.1
724C-21X-4, 59–61	190.29		3.63		30.2
724B-21X-3, 87–89	193.87		1.87		15.6
724C-22X-3, 76–78	198.56		6.69		55.7
724B-22X, CC (12–14)	200.57		2.08		17.3
724C-22X-5, 74–76	201.54		0.18		1.5
724C-23X-3, 98–100	208.48		2.32		19.3
724B-23X-3, 70–72	213.10		3.50		29.2
724B-23X-4, 0–1	213.90	9.19	5.68	3.51	47.3
724B-23X-5, 70–72	216.10		1.65		13.7
724B-23X-7, 20–22	218.60	5.70	0.21	5.49	1.8
724C-24X-4, 76–78	219.36		4.46		37.2
724B-24X-2, 35–37	220.85		4.72		39.3
724B-24X-4, 93–95	224.43		7.52		62.6
724B-24X-6, 78–80	227.28	9.20	1.88	7.32	15.7
724C-25X-4, 64–66	228.84		6.28		52.3
724B-25X-2, 47–49	230.67		6.64		55.3
724B-25X-4, 30–32	233.50		5.53		46.1
724B-25X-5, 0–1	234.70	7.82	5.88	1.94	49.0
724B-25X-6, 7–9	236.27		5.49		45.7
724C-26X-4, 55–57	238.45		5.51		45.9
724B-26X-2, 132–134	241.22		4.34		36.2
724B-26X-4, 4–6	242.94		5.39		44.9
724B-26X-6, 66–68	246.56		5.38		44.8
724C-27X-4, 58–60	247.98		4.25		35.4
724B-27X-2, 6–8	249.56		5.82		48.5
724B-27X-4, 65–67	253.15		5.08		42.3
724B-27X-6, 7–9	255.57		7.95		66.2

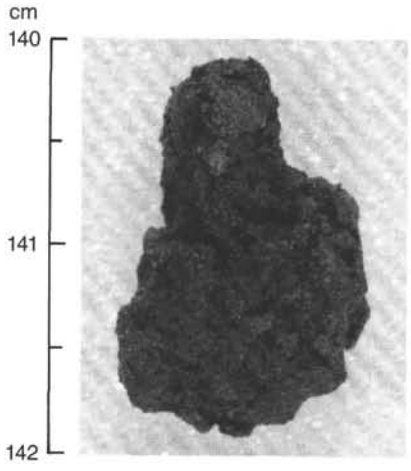

Figure 9. Black (5Y 2.5/1) apatite nodule from Sample 117-724B-5H, 141–142 cm.

Hole 724B, the preservation becomes poor whereas the abundance remains high in Samples 117-724C-19X, CC and 117-724C-20X, CC (165.9–185.2 mbsf). The decrease in nannofossil abundance mimics the pattern in Hole 724B, but abundance increases again in Sample 117-724C-22X, CC (204.5 mbsf) and remains high throughout the remainder of the hole, with moderate preservation (204.5–252.4 mbsf).

As at all of the other Leg 117 sites, the species diversity is comparatively low, and discoasters are not usually found in high concentrations.

Samples down to Samples 117-724A-2H-5, 105–106 cm (13.55 mbsf), 117-724B-1H, CC (7.0 mbsf), and 117-724C-1H, CC (2.8 mbsf) contain *Emiliania huxleyi* and are assigned to Zone NN21. Samples 117-724A-2H, CC to 117-724A-4H, CC (15.90–34.90 mbsf), 117-724B-2H, CC and 117-724B-3H, CC (7.0–25.9 mbsf), and 117-724C-2H, CC through 117-724C-4H, CC (2.8–31.2 mbsf) contain neither *E. huxleyi* nor *Pseudoemiliania lacunosa* and are assigned to Zone NN20. Samples 117-724A-5H, CC (44.5 mbsf), 117-724B-5H-1, 105–106 cm, through 117-724B-18X-3, 121–122 cm (36.45–165.21 mbsf), and 117-724C-5H, CC through 117-724C-17X, CC (31.2–156.3 mbsf) contain *P. lacunosa* and are assigned to Zone NN19. The following datums are recognized in Zone NN19 (see "Explanatory Notes" chapter, this volume), and additional information is tabulated in Table 4.

Datum 1: Uncertain
Datum 2: 2.8–9.4 mbsf (Core 117-724C-2H)
Datum 3: 31.2–40.8 mbsf (Core 117-724C-5H)
Datum 4: Uncertain
Datum 5: 60.2–69.8 mbsf (Core 117-724C-8X)
Datum 6: 60.2–69.8 msbf (Core 117-724C-8X)
Datum 7: 79.4–89.0 mbsf (Core 117-724C-10X)
Datum 8: 98.6–108.3 mbsf (Core 117-724C-12X)
Datum 9: Uncertain
Datum 10: 117.8–127.4 mbsf (Core 117-724C-14X)
Datum 11: 127.4–137.0 mbsf (Core 117-724C-15X)

Datum 11 marks the approximate position of the Pleistocene/Pliocene boundary. Neogene Samples 117-724B-18X, CC and 117-724B-19X, CC (170.7–180.0 mbsf) and 117-724C-18X, CC through 117-724C-22X, CC (165.9–204.5 mbsf) contain *Discoaster brouweri* as the only representative of the genus and thus are assigned to Zone NN18 (upper Pliocene). Sample 117-724B-20X, CC contains *Discoaster pentaradiatus* but not *Discoaster surculus* and, therefore, is assigned to Zone NN17. Samples 117-724B-21X, CC through 117-724B-25X, CC (199.7–238.4 mbsf) contain *D. surculus* but not *Reticulofenestra pseudoumbilica* and are assigned to Zone NN16. Because *D. surculus* was not found in Hole 724C, Samples 117-724C-23X, CC through 117-724C-25X, CC (214.1–233.4 mbsf) are assigned to Zones NN16–17. All sediments below Samples 117-724B-26X-1, 104–105 cm (239.44–257.7 mbsf) and 117-724C-26X, CC (242.9–252.4 mbsf) contain *R. pseudoumbilica* but not *Discoaster asymmetricus* and are assigned to uppermost lower Pliocene Zone NN15.

Traces of Cretaceous species such as *Cribrosphaerella ehrenbergii, Watznaueria barnesae, Micula decussata, Cretarhabdus* spp., *Prediscosphaera intercisa, Cretarhabdus loriei*, and *Microrhabdulus decoratus* are found throughout Holes 724B and 724C. Paleogene species such as *Cyclicargolithus floridanus, Cyclicargolithus abisectus*, and *Cribrocentrum reticulatum*, Eocene-Oligocene species *Sphenolithus predistentus*, and Miocene species *Discoaster deflandrei* are also found.

Radiolarians

Core-catcher samples from Hole 724B were examined for radiolarians. The first 19 cores (to 180.4 mbsf) are either barren or have a very sparse fauna (4 to 5 specimens per strewn slide). Diatoms are also absent from these samples.

Samples 117-724B-20X, CC to 117-724B-24X, CC (190.0–228.7 mbsf) contain a significant number of radiolarians, but species diversity is low. The assemblage closely resembles that found in the lowest part of Hole 723B, except for minor differences associated with an age difference between the radiolarian-rich sequences in the two holes. The last occurrence datum of *Stichocorys peregrina* occurs in Sample 117-724B-22X, CC (209.4 mbsf), marking the upper limit of the *Spongaster pentas* Zone. This species is the only tropical zonal marker found in Hole 724B. Radiolarian abundances decrease in Samples 117-724B-25X, CC and 117-724B-27X, CC (238.4–257.7 mbsf).

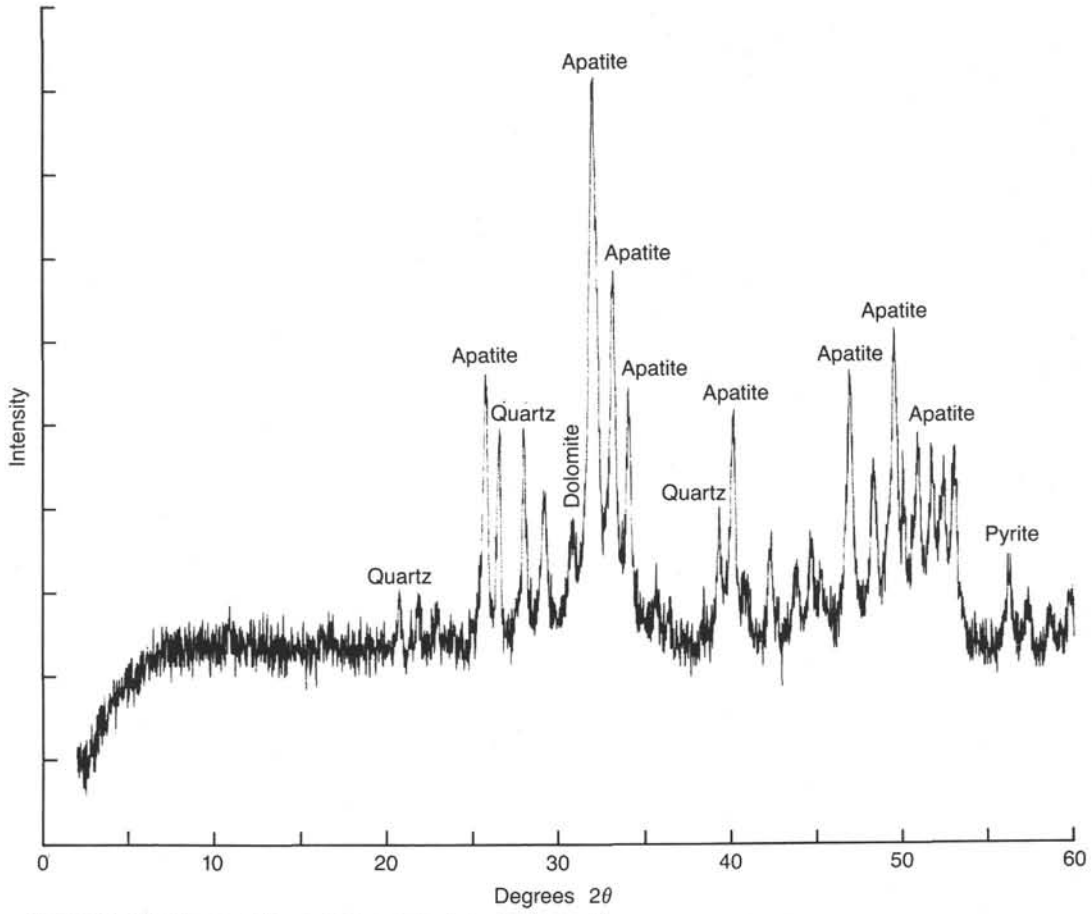

Figure 10. XRD trace of the apatite nodule shown in Figure 9.

Paleoenvironmental Implications

Ammonia beccarii is a well-known neritic benthic foraminiferal species that has a lower depth limit well above 350 m in the modern oceans. Site 724 is today located at a water depth of 593 m, whereas the presence (up to about 10% of the benthic foraminiferal fauna) of *A. beccarii* in the lower part of the sequence studied indicates either a subsiding sea-bottom caused by faulting or downslope transport of material from shallower areas. The uniformity of the color of the phosphorite found throughout the sequence indicates a single source for the material, and thus, we favor the idea of a subsiding sea bottom. Different colors of phosphorite found at one location usually indicate transportation of material from various sources and different ages (redeposition—thanatocoenosis), whereas color uniformity indicates a single source (biocoenosis).

The varying preservation states of the planktonic foraminifers and coccoliths are thought to be related to the reducing conditions in the oxygen-minimum zone, which enhance carbonate dissolution. Reduced planktonic foraminiferal faunas are present in Samples 117-724B-17X, CC through 117-724B-25X, CC (161.0–238.4 mbsf), which are dominated by robust thick-walled species. With the decline of the calcareous fauna is a concomitant increase in abundance of the siliceous fauna.

The nannofossil genus *Helicosphaera* is thought to prefer upwelling areas. This genus is especially numerous in Samples 117-724B-10X, CC (93.4 mbsf), 117-724B-15X, CC (141.7 mbsf), 117-724B-17X, CC (161.0 mbsf), and 117-724C-18X, CC (165.9 mbsf). *Coccolithus pelagicus*, a species known to inhabit cold waters, is found in Samples 117-724B-15X, CC through 117-724B-17X, CC (141.7–161.0 mbsf; lowermost Pleistocene to uppermost Pliocene) and 117-724C-15X, CC through 117-724C-19X, CC (137.0–175.2 mbsf; lowermost Pleistocene to uppermost Pliocene). Interestingly, the large numbers of *Helicosphaera* spp. are always associated with high abundances of *C. pelagicus*, but not all Site 724 samples with high numbers of *C. pelagicus* contain *Helicosphaera* spp. in unusually high concentrations.

PALEOMAGNETISM

Site 724 is at 18°28′N, 57°47′E in a water depth of about 600 m on the Oman margin. Holes 724A, 724B, and 724C were cored to depths of 44.8, 257.7, and 252.4 mbsf, respectively. The lithology consists mainly of calcareous clayey silt.

Magnetic Measurements

The archive halves of five APC cores from Hole 724A (Cores 117-724A-1H through 117-724A-5H) were measured on the pass-through cryogenic magnetometer after alternating field (AF) demagnetization at 5 mT. As for Site 723, the inclinations generally correspond to the expected axial dipole value (33.7°).

Our efforts in measuring discrete samples with the MINISPIN fluxgate spinner magnetometer and the Schonstedt AF demagnetizer proved more fruitful than at Site 723. We selected a peak AF of 5 or 10 mT (depending on the initial intensity) for blanket demagnetization. Stepwise AF demagnetization of samples from Hole 724B suggested that the characteristic magnetization was detectable after AF cleaning at peak fields of 5–10 mT (Figs. 14 through 17). Intensities after AF demagnetization were generally higher than at Site 723: around 1 mA/m down to about 190 mbsf, below which they drop to around 0.1 mA/m. The arithmetic mean intensity is 0.7 mA/m. Figure 18 shows

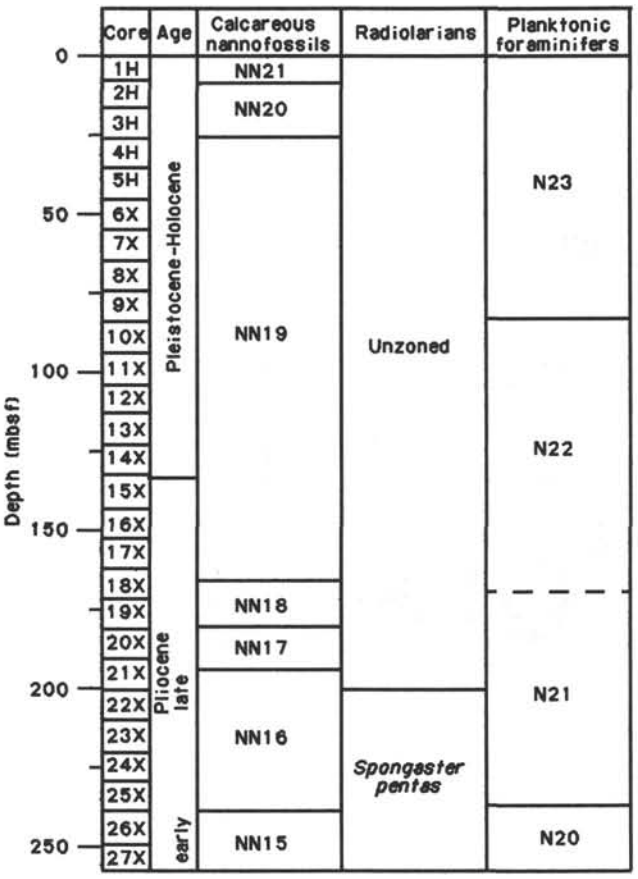

Figure 11. Calcareous nannofossil, radiolarian, and planktonic foraminifer biostratigraphy of Hole 724B.

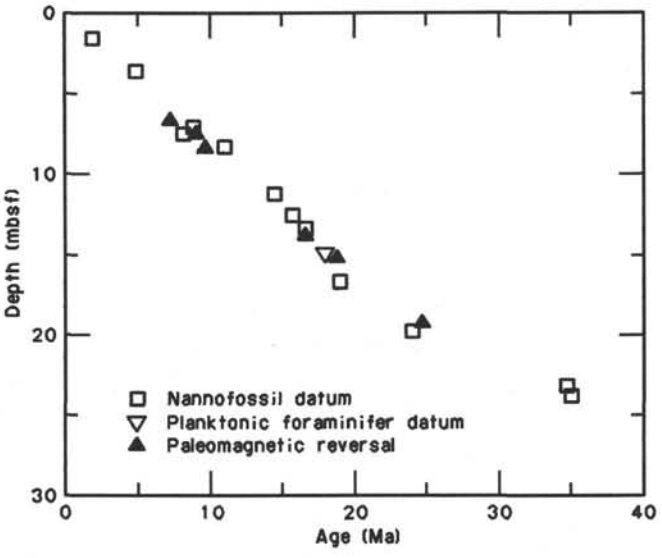

Figure 12. Age-depth plot for Site 724. Events are from Holes 724A and 724B (see Table 4 for a detailed list of events).

that the inclination values of both normally and reversely magnetized specimens are distributed around the expected value for the site.

Downhole plots of declination, inclination, and intensity after AF demagnetization are shown in Figures 19 through 21; points with circular standard deviation (CSD) values greater than 40° are excluded. Samples from Hole 724A, ranging from 0 to 44.5 mbsf, all have downward inclinations (Fig. 19). The two deeper holes, 724B (Fig. 20) and 724C (Fig. 21), show consistent magnetic polarity records for the Pliocene and Pleistocene. At least six polarity transitions are evident in the records, and we tentatively recognize the Chron C1/C1r (Brunhes/Matuyama Chronozone) boundary and Chron C1r-1 (Jaramillo Subchronozone) and more confidently recognize Chron C2 (Olduvai Subchronozone) and the beginning of Chron C2A (Gauss Chronozone). Table 5 lists the core intervals, depths below seafloor, and estimated ages of these transitions. The horizons of the polarity transitions are both consistent between the two holes and concordant with calcareous nannofossil biostratigraphy. Our age estimates give a sedimentation rate of about 80 m/m.y. for this site during the Pleistocene.

Two samples from the 47.6–49.2 mbsf interval of Hole 724B (Samples 117-724B-6X-2, 115–117 cm, and 117-724B-6X-3, 115–117 cm) have negative inclinations, although we assign this interval to the Brunhes Chronozone. No negative inclinations are apparent within the same interval in Hole 724C; however, we did observe reversely magnetized Brunhes specimens in Core 117-723A-9H (see "Paleomagnetism" section, "Site 723" chapter). It is possible that this genuinely reflects geomagnetic field behavior; however, the quality of the paleomagnetic data and the lack of sufficiently tight age control inhibit attempts at correlation with previously suggested geomagnetic events and excursions within the Brunhes.

Magnetic Susceptibility

The volume magnetic susceptibility of Holes 724A, 724B, and 724C was measured on the Bartington Instruments M.S. 1 whole-core susceptibility sensor at 0.1 sensitivity and low-frequency (0.47-kHz) settings. As a result of gas expansion in the deepest cores, the volume magnetic susceptibility of split-core sections was measured from Cores 117-724B-16X to 117-724B-26X and 117-724C-18X to 117-724C-27X. Values obtained during these measurements were multiplied by two during processing. Measurements were made on all cores at 10-cm intervals for a total of 425, 1582, and 1911 measurements for Holes 724A, 724B, and 724C, respectively. Susceptibility values ranged from 50×10^{-6} to 125×10^{-6} and averaged about 100×10^{-6} volume SI units, which is slightly higher than observed at Site 723 and slightly lower than at Sites 722 and 721. To a first-order approximation, the intersite differences in mean susceptibility are inversely related to differences in the relative accumulation rates, which suggests that the variability between sites is due to dilution by nonmagnetic components. At this stage, however, we are unsure as to whether the downhole variability is due to changes in the fluxes of predominantly terrigenous (magnetic) or biogenic (nonmagnetic) components (see "Paleomagnetism" section, "Site 723" chapter).

The susceptibility data for Cores 117-724A-1H to 117-724A-5H, 117-724B-1H to 117-724B-5H, and 117-724C-1H to 117-724C-5H (0–~45 mbsf) are quite similar, and interhole correlations are generally accurate to within ~5 to 10 cm (Fig. 22). Anomalously high values that do not correlate between holes can be attributed to short intervals contaminated by pipe rust and other magnetic contaminants that occur at the core boundaries. Using the Brunhes-Matuyama Chronozone paleomagnetic datums for Holes 724A and 724B (Table 5), the age interval represented by these correlated sequences is approximately 500,000 yr.

Interhole correlations below the limit of APC recovery in Holes 724B and 724C (>45 mbsf) are considerably less detailed. Most of the correlations can be made for gross features only. Although XCB recovery was quite high, the recovered sediments were generally too disturbed for detailed susceptibility

Table 4. Stratigraphic listing of faunal events and paleomagnetic reversals for Holes 724A and 724B.

Event	Core, section, interval (cm)	Depth (mbsf)	Age (Ma)	Source of age	Notes
B *Emiliania huxleyi*	724A-2H-5, 105–106, to 724A-2H, CC	13.55 15.90	0.19	3	
T *Pseudoemiliania lacunosa*	724A-4H, CC 724B-5H-1 105–106	34.90 36.45	0.49	3	
Bruhnes/Matuyama	724B-8X-1, 105–107 724B-8X-2, 105–107	65.45 66.95	0.73	6	
B *Gephyrocapsa parallela*	724B-8X-3, 110–111 724B-8X-5, 100–101	68.50 71.40	0.89	4	North Atlantic data
T Jaramillo	724B-8X-5, 94–96 724B-9X-1, 114–116	71.34 75.14	0.91	6	
T *Reticulofenestra* sp. A	724B-8X, CC, 724B-9X-1, 105–106	74.00 75.05	0.82	3	
T *Gephyrocapsa* "large"	724B-9X-5, 105–106 724B-9X, CC	81.05 83.70	1.10	4	North Atlantic data Long axis greater than 6 μm
B Jaramillo	724B-9X-5, 114–116 724B-10X-1, 105–107	81.18 84.75	0.98	6	
T *Helicosphaera sellii*	724B-12X-1, 135–136 724B-12X-3, 105–106	104.35 107.05			No good published age; event appears to be diachronous
T *Calcidiscus macintyrei*	724B-12X-5, 100–101 724B-12X, CC	110.00 112.70	1.45	6	
B *Gephyrocapsa oceanica*	724B-14X-1, 110–111 724B-14X-3, 104–105	123.50 126.44	1.57	4	North Atlantic data
B *Gephyrocapsa caribbeanica*	724B-14X, CC 724B-15X-1, 103–104	132.00 133.03	1.66	4,8	North Atlantic age consistent with Italian-type section
T Olduvai	724B-15X-2, 68–70 724B-16X-1, 108–110	134.18 142.78	1.66	6	
T *Globigerinoides extremus*	724B-16X-4, 65–67 724B-16X, CC	146.85 151.40	1.80	6	*G. obliquus extremus* in Berggren et al., 1985
B Olduvai	724B-16X-6, 116–118 724B-17X-1, 127–129	150.36 152.67	1.88	6	
T *Discoaster brouweri*	724B-18X-3, 121–122 724B-18X-5, 105–106	165.21 168.05	1.9	6	
Matuyama/Gauss	724B-20X-6, 108–110 724B-21X-2, 141–143	188.98 192.91	2.47	6	
T *Discoaster surculus*	724B-21X-3, 105–106 724B-21X, CC	194.05 199.70	2.4	6	
T *Sphenolithus abies*	724B-25X-1, 135–135 724B-25X-3, 135–136	230.05 233.05	3.47	6	
T *Reticulofenestra pseudoumbilica*	724B-25X, CC 724B-26X-1, 104–105	238.40 239.44	3.5	6	

Note: T = upper limit of event and B = lower limit. Sources of ages are: 3 = oxygen isotope data for Site 723 (N. Niitsuma, unpubl. data); 4 = Takayama and Sato, 1987; 6 = Berggren et al., 1985; and 8 = Sato et al., in press.

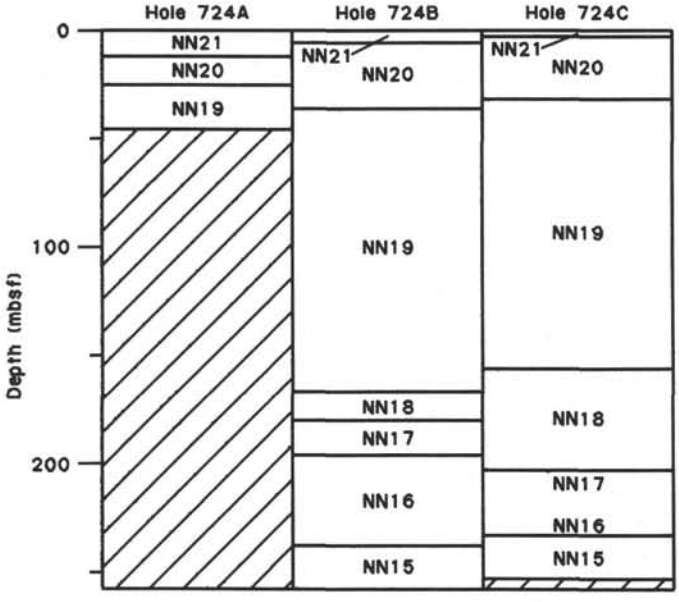

Figure 13. Correlation of calcareous nannofossil zones in Holes 724A, 724B, and 724C.

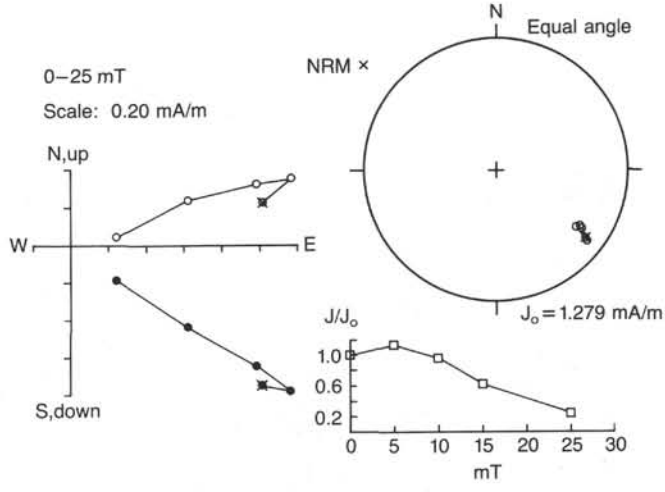

Figure 14. Result of stepwise AF demagnetization for Sample 117-724B-14X-2, 121–123 cm.

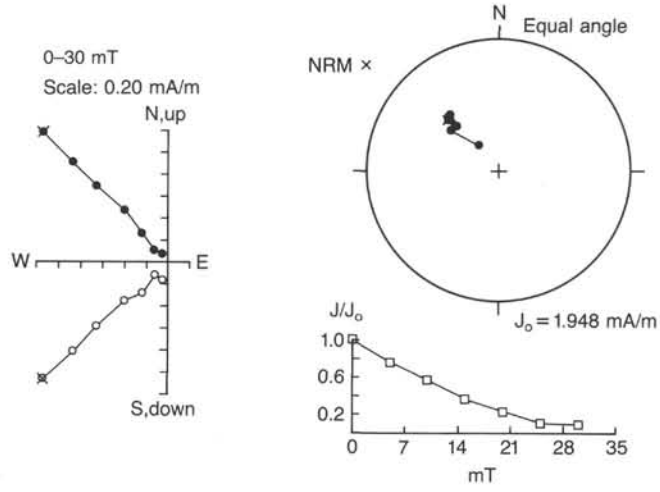

Figure 15. Result of stepwise AF demagnetization for Sample 117-724B-16X-1, 108–110 cm.

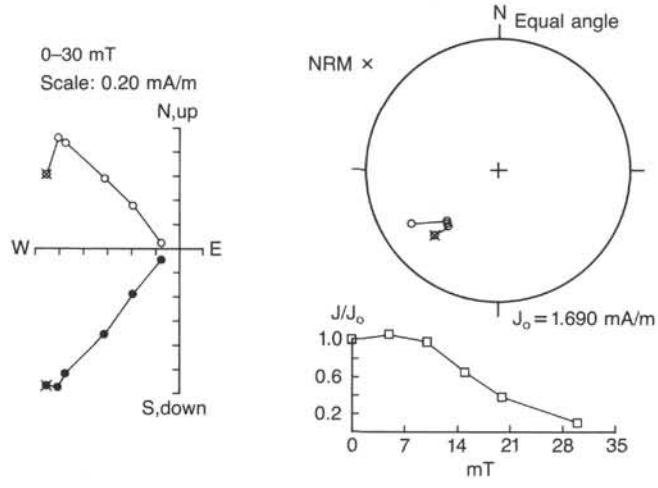

Figure 16. Result of stepwise AF demagnetization for Sample 117-724B-17X-1, 127–129 cm.

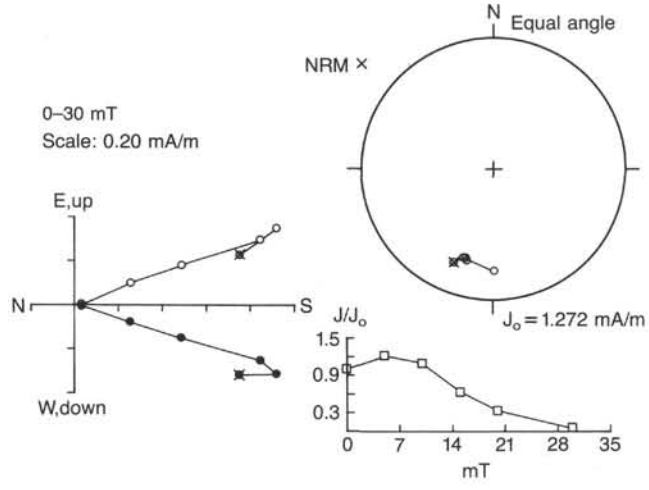

Figure 17. Result of stepwise AF demagnetization for Sample 117-724B-18X-5, 110–112 cm.

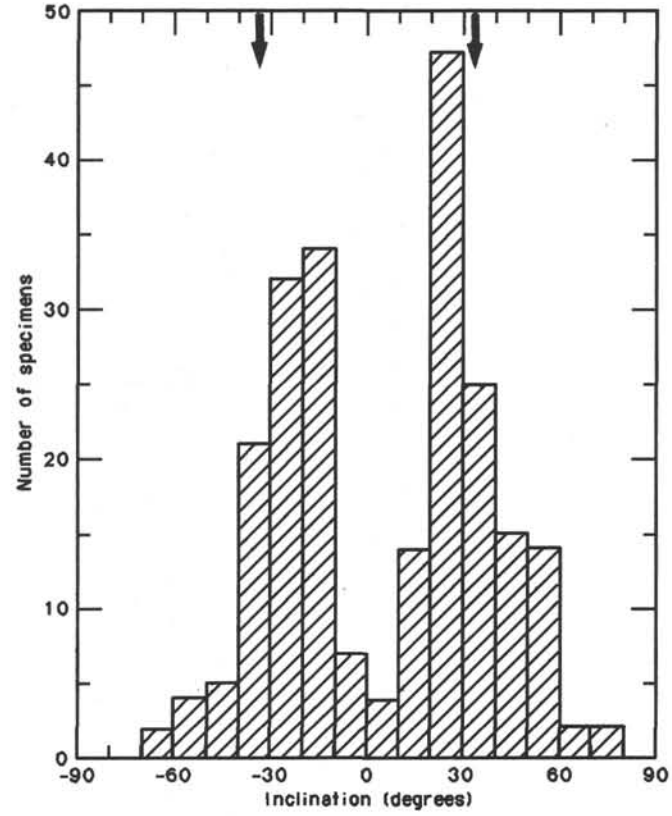

Figure 18. Histogram of magnetic inclination values from Site 724. Arrows show the values expected from the geocentric axial dipole field (33.7°).

correlations. Tentative correlations between Holes 724B and 724C are shown in Figure 23. Detailed interhole correlations based on these data and lithologic marker layers are presented in the "Interhole Correlations" section of this chapter.

Intersite correlations between the two Oman margin sites drilled thus far (723 and 724) are shown in Figure 24. The data are from the Brunhes Chronozone only (<0.73 Ma). The agreement between Sites 723 and 724 is remarkably good despite the differences in core quality, site location (~40 km apart), water depth (800 vs. 570 m), and accumulation rates (~175 vs. ~80 m/m.y). Moderate stretch and compression of the Brunhes Chronozone susceptibility record is apparent at both sites, and there is some indication of missing sediment or condensed sedimentation at ~8 and ~31 mbsf in Hole 724C. Ultimately, we hope to construct detailed intersite correlations for all of the suitable Oman margin and Owen Ridge sites.

ACCUMULATION RATES

Sedimentation rates for Site 724 are based on the magnetostratigraphic and biostratigraphic data listed in Table 4 and shown in Figure 25. Because of the high quality of the data, eight nannofossil datums, with ages from oxygen isotope stratigraphy (N. Niitsuma, unpubl. data) and Berggren et al. (1985) are favored for determination of the sedimentation rates at Site 724 over the last 3.5 m.y. Rates are determined at other Leg 117 sites using these same events to allow between-site comparisons of sediment accumulation.

Over the last 2.4 m.y. at Site 724, the mean sedimentation rate varied between 59 and 142 m/m.y. (Table 6), with an overall mean of 80 m/m.y. This is less by a factor of 2 than the sedimentation rate at nearby Site 723, which is in the center of the

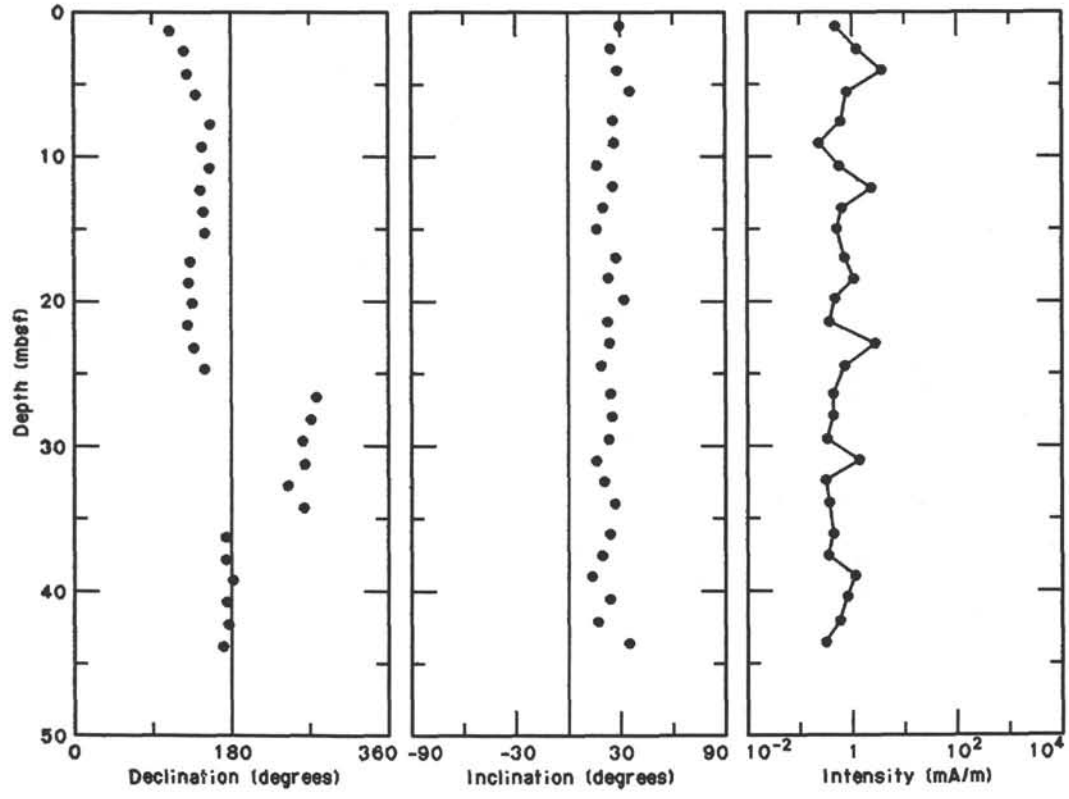

Figure 19. Magnetic declination (relative values), inclination, and intensity profiles for Hole 724A, obtained after AF demagnetization.

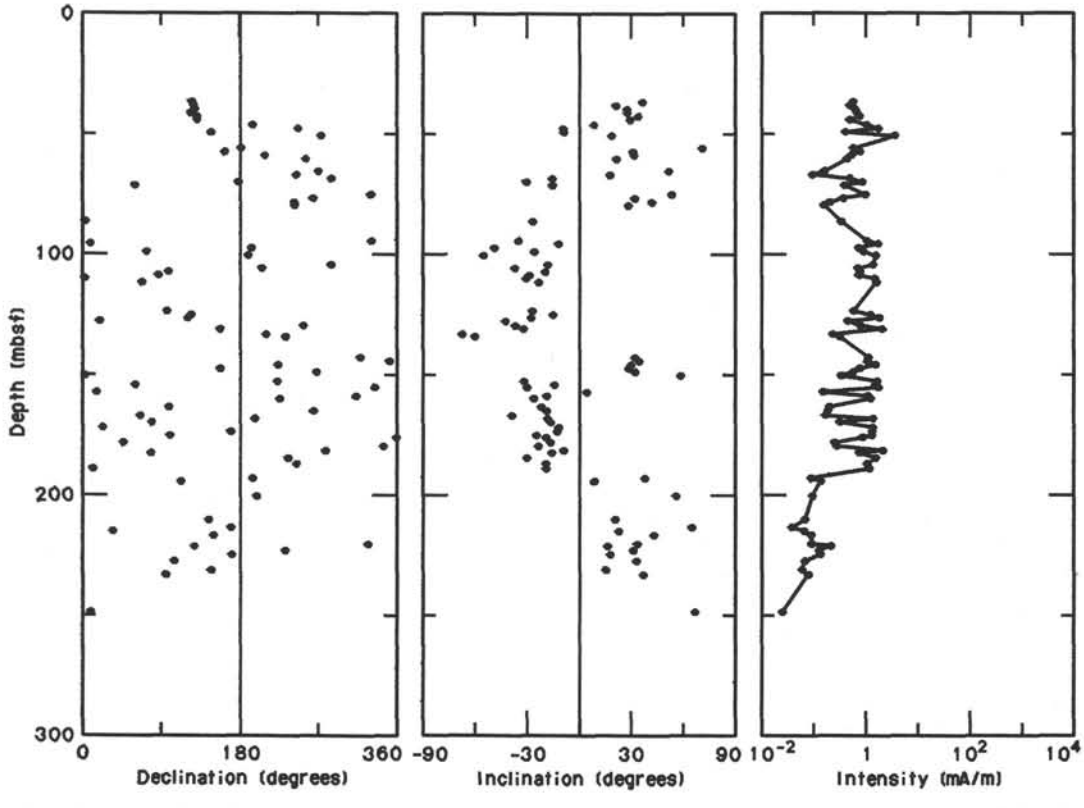

Figure 20. Magnetic declination (relative values), inclination, and intensity profiles for Hole 724B, obtained after AF demagnetization.

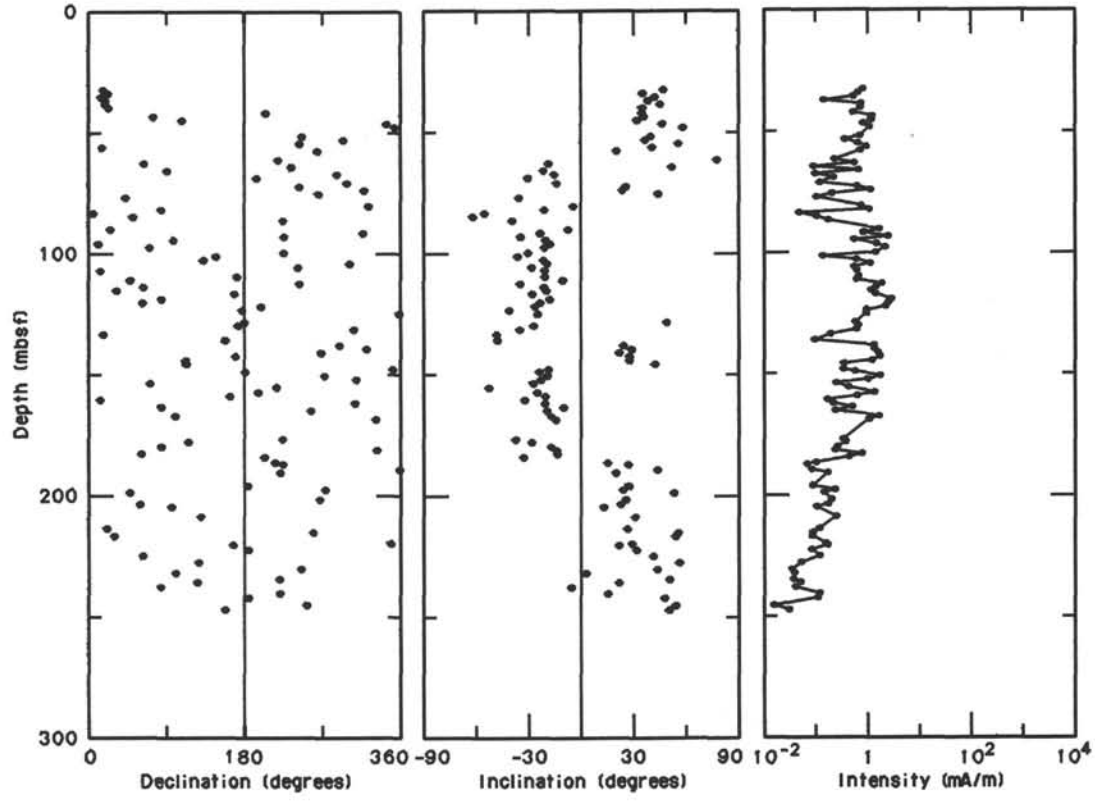

Figure 21. Magnetic declination (relative values), inclination, and intensity profiles for Hole 724C, obtained after AF demagnetization.

Table 5. Polarity transitions in Holes 724B and 724C.

Boundary (Age)	Sample interval	Depth (mbsf)
Brunhes/Matuyama	724B-8X-1, 105 cm, to 724B-8X-2, 105 cm	65.45-66.95
C1/C1r (0.73 Ma)	724C-8X-1, 119 cm, to 724C-8X-2, 119 cm	61.39-62.89
Top of Jaramillo	724B-8X-5, 94 cm, to 724B-9X-1, 114 cm	71.34-75.14
C1r/C1r-1 (0.91 Ma)	724C-9X-1, 119 cm, to 724C-9X-2, 119 cm	70.99-72.49
Bottom of Jaramillo	724B-9X-5, 114 cm, to 724B-10X-1, 105 cm	81.18-84.75
C1r-1/C1r (0.98 Ma)	724C-9X-4, 119 cm, to 724C-9X-5, 119 cm	75.49-76.99
Top of Olduvai	724B-15X-2, 68 cm, to 724B-16X-1, 108 cm	134.18-142.78
C1r/C2 (1.66 Ma)	724C-15X-6, 100 cm, to 724C-16X-1, 110 cm	135.90-138.10
Bottom of Olduvai	724B-16X-6, 116 cm, to 724B-17X-1, 127 cm	150.36-152.67
C2/C2r (1.88 Ma)	724C-16X-6, 118 cm, to 724C-17X-1, 140 cm	145.68-148.00
Matuyama/Gauss	724B-20X-6, 108 cm, to 724B-21X-2, 141 cm	188.98-192.91
C2r/C3 (2.47 Ma)	724C-20X-6, 106 cm, to 724C-21X-1, 117 cm	184.06-186.37

upper slope basin. Prior to 2.4 m.y. at Site 724, a lower rate of accumulation (35 m/m.y.) is associated with a greater abundance of organic-carbon-rich, laminated diatomaceous clayey silts (lithologic facies II).

The mass accumulation of calcium carbonate, organic carbon, and noncarbonate sediment components is calculated from average values between the nannofossil datums (Table 6 and Fig. 26). The rate of bulk sediment accumulation is approximately 12 g/cm^2/1000 yr, lower by a factor of 2 than that at Site 723, and calcium carbonate accounts for more than one-half of the mass accumulated. Preliminary shipboard data suggest that a significant part of the bulk carbonate accumulation is detrital material (see "Lithostratigraphy" section, this chapter). Therefore, carbonate accumulation reflects both pelagic and terrigenous sources. In comparison to nearby Site 723, organic carbon accumulation and concentration at Site 724 (Table 6) are significantly lower. These differences are only partly consistent with the positive correlation of sedimentation rate and organic matter preservation (see Müller and Suess, 1979).

PHYSICAL PROPERTIES

Physical-property measurements at Site 724 were limited by extensive gas-related sediment expansion. Discrete samples were taken from the least disturbed portions of cores for measurement of index properties (wet-bulk density, porosity, and grain density). Vane shear strength was determined only for APC cores of Hole 724A. Wet-bulk density and compressional-wave velocity were measured for the most coherent whole-round core sections with the GRAPE and *P*-wave logging systems. Reliable data acquisition with these systems was limited to the interval between the seafloor and 65 mbsf. Compressional-wave velocity could not be measured with the Hamilton Frame because of the inability to transmit a signal through the expanded sediment. All techniques and equipment used are described in the "Explanatory Notes" chapter.

Index Properties

Variation of index properties in Holes 724A, 724B, and 724C is primarily controlled by changes in sediment texture and composition. The two sediment types identified at Site 724, calcareous clayey silt and laminated diatomaceous clayey silt, are distinguishable on the basis of their physical properties; however, changes between the sediment types are gradational. Index properties measurements for Holes 724A, 724B, and 724C are listed in Table 7.

In the uppermost part of the section at Site 724 (0 to 35 mbsf) grain-size variation is responsible for wide variation in porosity (65% to 41%), water content (46% to 24%), and wet-bulk density (1.63 to 1.96 g/cm^3) (Fig. 27). Sand-rich intervals are characterized by porosities between 50% and 46% and wet-bulk densities between 1.87 to 1.96 g/cm^3. In the finer-grained

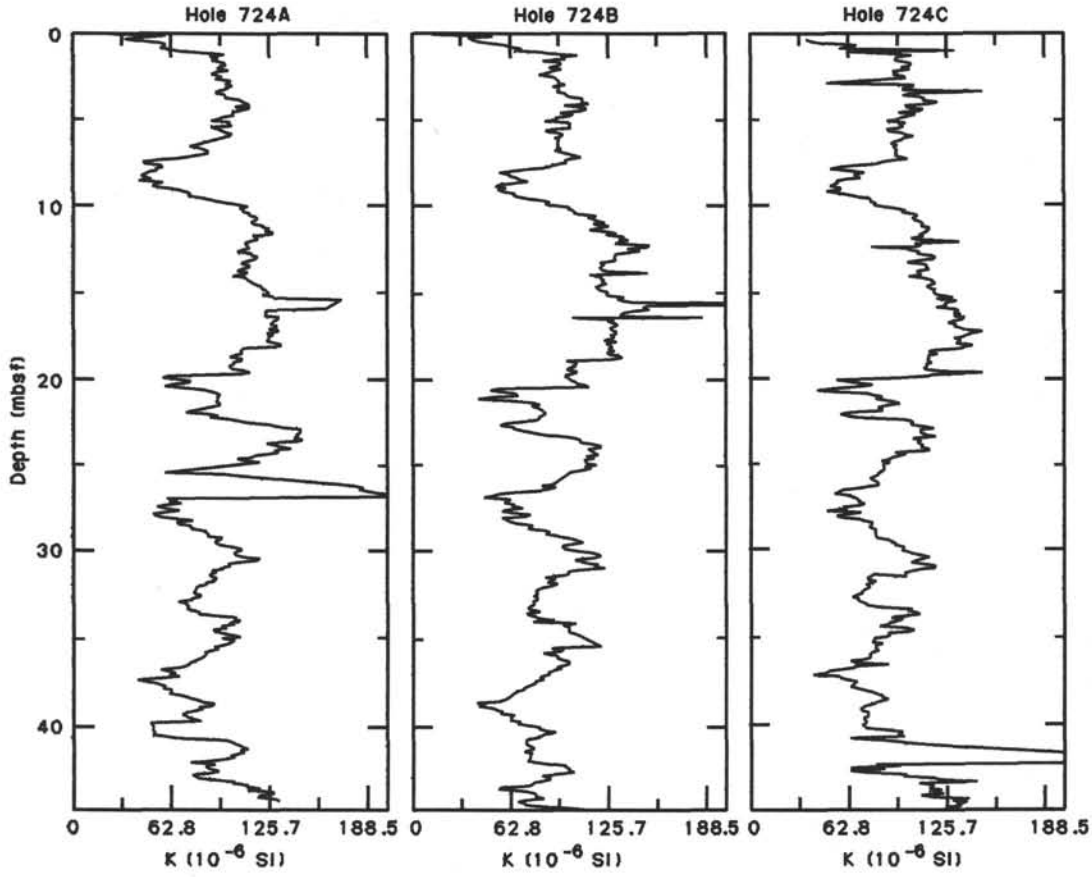

Figure 22. Plots of volume magnetic susceptibility data for 0 to 45 mbsf, Holes 724A, 724B, and 724C. These data were measured on the the first five APC cores of each hole.

sediments, porosity decreases from 62% near the seafloor to 54% at 35 mbsf. The wet-bulk density of these sediments increases from 1.68 to 1.82 g/cm^3 over the same interval.

Between 35 and 185 mbsf, porosity and water content are nearly constant at average values of 55% and 32%, respectively. Below 110 mbsf the variation of these averages is markedly reduced. The change in the degree of porosity variation at 110 mbsf roughly coincides with the disappearance of foraminifers in the sediments. Greater variation of porosity and water content probably reflect textural differences associated with the presence of foraminifers, with foraminifer-bearing sediments typically displaying lower porosity than finer-grained sediments. In the interval between 35 and 185 mbsf, grain density decreases uniformly from 2.73 to 2.55 g/cm^3 and is responsible for a decrease in wet-bulk density from 1.82 g/cm^3 to approximately 1.70 g/cm^3. The decreasing grain density coincides with a general trend of increasing abundance of organic matter and decreasing abundance of calcium carbonate (see "Lithostratigraphy" section).

Low grain density and wet-bulk density and varying porosity and water content characterize the interval between 185 and 230 mbsf. This depth range coincides with the principal occurrence of the diatomaceous clayey silts and dark, organic-rich clayey silts. The highest porosity (73%) and water content (51%) and the lowest wet-bulk density (1.48 g/cm^3) at Site 724 were measured for a sample from a diatom-rich layer at 213.1 mbsf (Sample 117-724B-23X-3, 70–72 cm). The grain density of this sample is low (2.48 g/cm^3) as a consequence of the low density of opal; however, the lowest grain densities (2.32 to 2.47 g/cm^3) are displayed by the dark, organic-rich layers. The high water content and porosity of the diatom-rich sediment are a reflection of the water-retaining attributes of siliceous microfossils. A positive correlation also exists between water content and organic matter abundance, as evidenced by the inverse relationship between water content (and porosity) and grain density in the interval between 185 to 230 mbsf.

Below 230 mbsf there is an insufficient thickness of sediments to document any consistent trends in porosity, water content, and wet-bulk density. Grain density displays a relatively uniform pattern of increase with depth, from 2.56 g/cm^3 at 230 mbsf to 2.74 g/cm^3 near the bottom of Hole 724B (Fig. 27). Foraminifers increase in abundance in this interval, and their reappearance is most likely responsible for the increase in grain density and variation in porosity, water content, and wet-bulk density.

GRAPE and *P*-Wave Logs

Determination of wet-bulk density by the GRAPE and compressional-wave (*P*-wave) velocity with the *P*-wave logger (PWL) was limited by sediment expansion. Continuous GRAPE data were obtained through Cores 117-724B-9X (83.7 mbsf) and 117-724C-9X (79.4 mbsf). In both holes, below approximately 65 mbsf the quality of the data decreases and the density is less than that determined for discrete samples as a consequence of the small fractures associated with sediment expansion. The GRAPE records display a cyclic variation similar to that at Site 723, except that at Site 724 the cycles are roughly half as thick. A tentative correlation of the features of the GRAPE records from Sites 724 and 723 is shown in Figure 28.

Velocity determinations with the PWL represent the only velocity measurements at Site 724. Velocity logs were obtained to depths of 48 mbsf in Hole 724B and 46 mbsf in Hole 724C. The

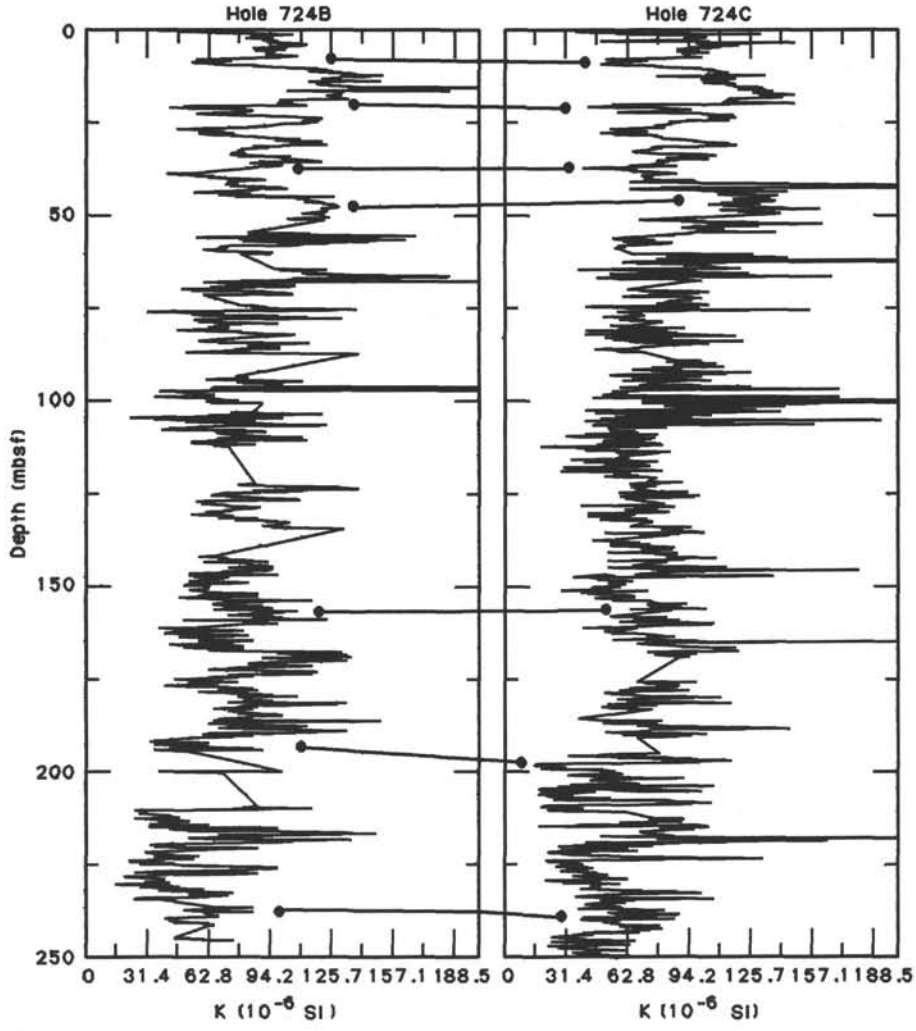

Figure 23. Plots of volume magnetic susceptibility of Holes 724B and 724C with tentative correlation of layers indicated.

measured velocities range from 1540 to 1680 m/s (Fig. 29) and display a pattern of cyclic variation that mimics that of the GRAPE wet-bulk density records.

Vane Shear Strength

Five measurements of vane shear strength were made on cores from Hole 724A (Table 7). The shear strengths varied from 10.29 kPa at 3.9 mbsf to 41.35 kPa at 30.9 mbsf. Below 40 mbsf, expansion-related disturbance made the sediment unsuitable for shear-strength determination.

INORGANIC GEOCHEMISTRY

At Site 724, 14 interstitial-water samples (two from Hole 724A, seven from Hole 724B, and five from Hole 724C) were collected by squeezing. No *in-situ* samples were collected at this site. All analytical results are listed in Tables 8 and 9 and presented in Figure 30. Note that the profiles were compiled by stacking the data sets from all three holes; this procedure may introduce some scatter if the specified depths below seafloor do not strictly correlate.

Salinity, Chloride, and pH

The concentration profiles of salinity, chloride, and pH are shown in Figure 30. As at previous sites, the salinity decrease between 0 and 100 mbsf can be attributed to the loss of sulfate and magnesium from solution (as discussed in the following text).

The chloride profile shows a distinct maximum between the top of the hole and ~80 mbsf, which is similar to the distribution of Cl^- at Site 725. At both sites the maximum is centered in sediments deposited in the mid-Pleistocene, which suggests that bottom water at that time was significantly more saline, at least on this part of the Oman margin. The Cl^- profiles at both sites have been subsequently smoothed by diffusion.

The pH measurements reported in Table 8 and plotted in Figure 30 should be considered to be approximate values only. As at other margin sites, degassing of CO_2 while the pH electrode was immersed in the pore fluid caused a severe upward drift of successive pH measurements; accuracy is therefore poor.

Sulfate and Alkalinity

The sulfate concentration decreases sharply over the upper 50 m of the cored section (Fig. 30), with a gradient (−0.5 mmol/L per m) comparable to that observed at Site 723. However, in contrast to the absence of sulfate at depth at Site 723, SO_4^{2-} is detectable in minor concentrations throughout the deeper part of the cored sequence at Site 724 (Table 8). This may reflect the cessation of sulfate reduction at depth.

Alkalinity increases steadily with depth (Fig. 30). The con-

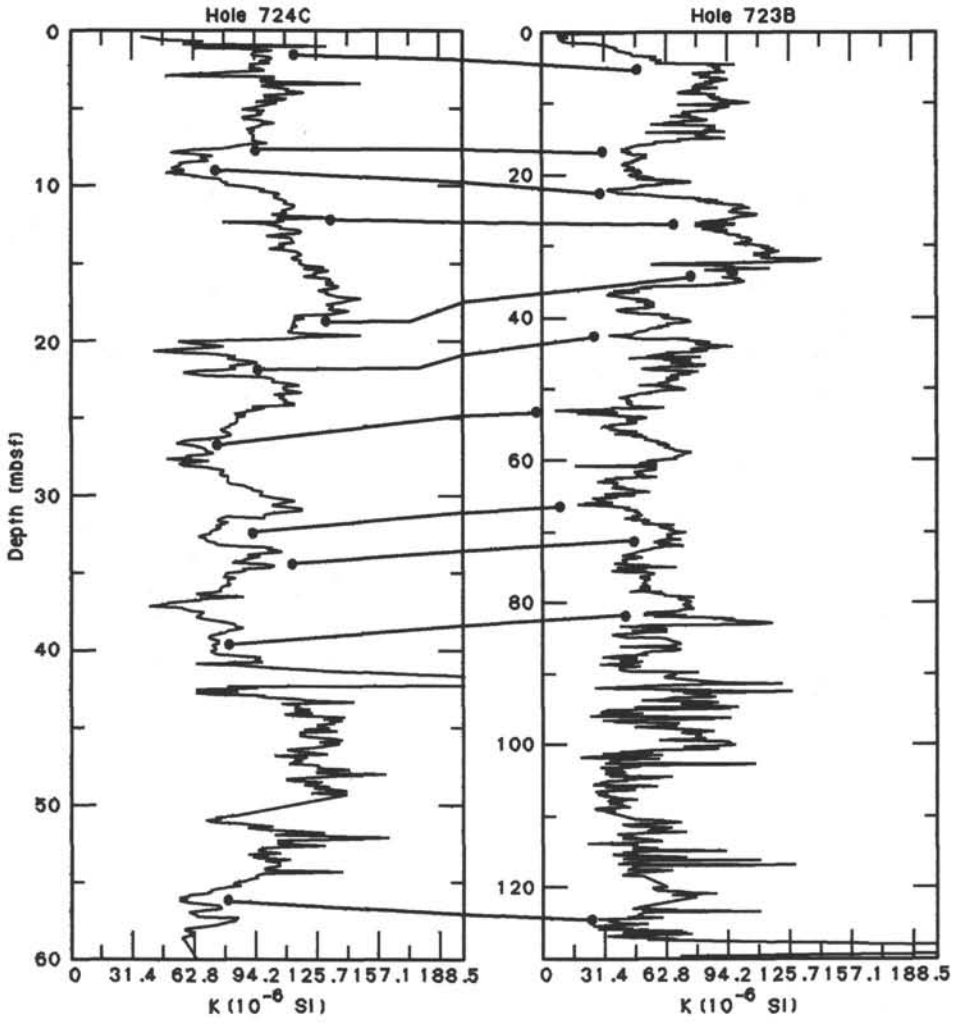

Figure 24. Brunhes Chronozone susceptibility correlations of Holes 723B and 724C from the Oman margin.

centration at 50 mbsf, where sulfate is depleted to <1 mmol/L, is about 13 mmol/L, ~ 40 mmol/L less than would be produced by the reduction of 27 mmol/L of SO_4^{2-}. The deficit can be explained by the precipitation of authigenic carbonate minerals, as at previous sites. Below 50 mbsf, the alkalinity increase can be entirely accounted for by the continuing production of ammonia (see the following text) as organic matter is degraded during methanogenesis; methane is abundant at depth at this site (see "Organic Geochemistry" section, this chapter).

Calcium and Magnesium

Calcium and magnesium concentrations both decrease with depth (Fig. 30), with the steepest negative gradients occurring in the top 50 m. The maximum in the Mg/Ca ratio at 9 mbsf can be accounted for by the initial precipitation of calcite followed by the occurrence of dolomitization below ~ 10 mbsf. The profiles indicate that most of the precipitation of authigenic carbonates occurs in the top 50 m, which is consistent with the alkalinity deficit. Indeed, ~ 23 mmol/L of Mg^{2+} and 3 mmol/L of Ca^{2+} are consumed from solution in this upper zone to account for 60% of the "missing" alkalinity: presumably the rest of the alkalinity deficit can be attributed to the precipitation as calcite of calcium released to solution during the dolomitization of preexisting biogenic $CaCO_3$.

Ammonia, Phosphate, and Silica

Concentration profiles of these interstitial-water constituents are shown in Figure 30. Ammonia reaches relatively high concentrations, up to ~ 20 mmol/L, in the lower 200 m of the cored section, which reflects ongoing degradation of organic matter at depth. However, the concentrations in the top 50 m are lower than would be expected given the reduction of ~ 27 mmol/L of SO_4^{2-}, suggesting that several mmol/L of NH_4^+ have been adsorbed by clay minerals. We cannot determine if such uptake continues at greater depth.

Phosphate concentrations are rather variable at this site, partly as a result of analytical interference from dissolved sulfide (see "Explanatory Notes" chapter). The measured levels are again low, indicating that apatite must be precipitating in the sediments at Site 724; such authigenesis appears to be a universal phenomenon in organic-rich Arabian Sea sediments.

Dissolved silica increases with depth through the upper 50 m to values approaching the solubility of biogenic opal. Highest concentrations occur at ~ 80 mbsf and below 200 mbsf (Table 8),

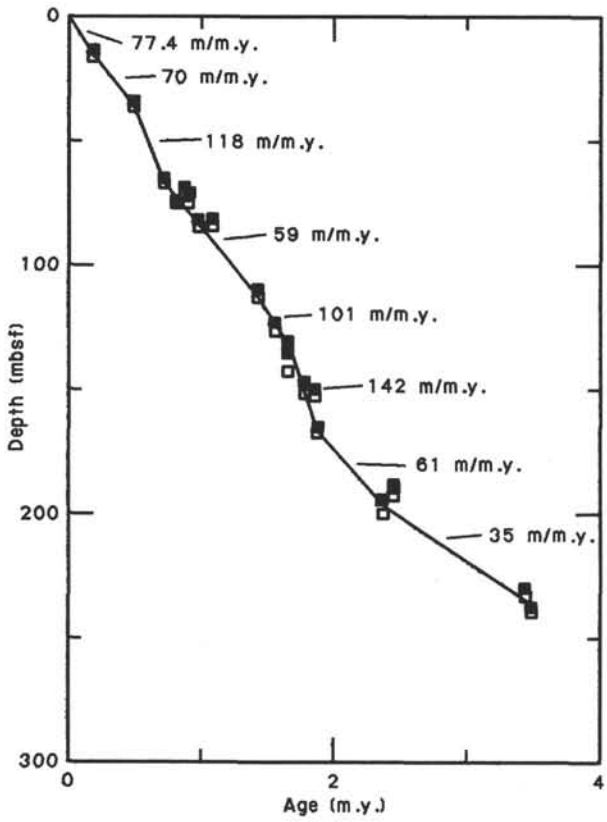

Figure 25. Age-depth plot of stratigraphic datums listed in Table 4. The solid and open boxes are the upper and lower boundaries of each datum, respectively. Indicated sedimentation rates are calculated between reliable nannofossil datum levels.

indicating zones of sediment relatively enriched in opal. High abundances of diatoms were observed in smear slides in Cores 117-724B-22X and 117-724B-23X at ~200–220 mbsf (see "Lithostratigraphy" section), which agrees with the pore-water results.

Dissolved Organic Carbon

The relative abundance of dissolved organic carbon (Table 9; see "Inorganic Geochemistry" section, "Site 723" chapter, for an explanation) in Site 724 pore waters is shown in Figure 30. The profile appears to reflect the general distribution of sedimentary organic carbon in the upper 100 m of the section but is poorly correlated in the lower 150 m. We do not know why this is the case.

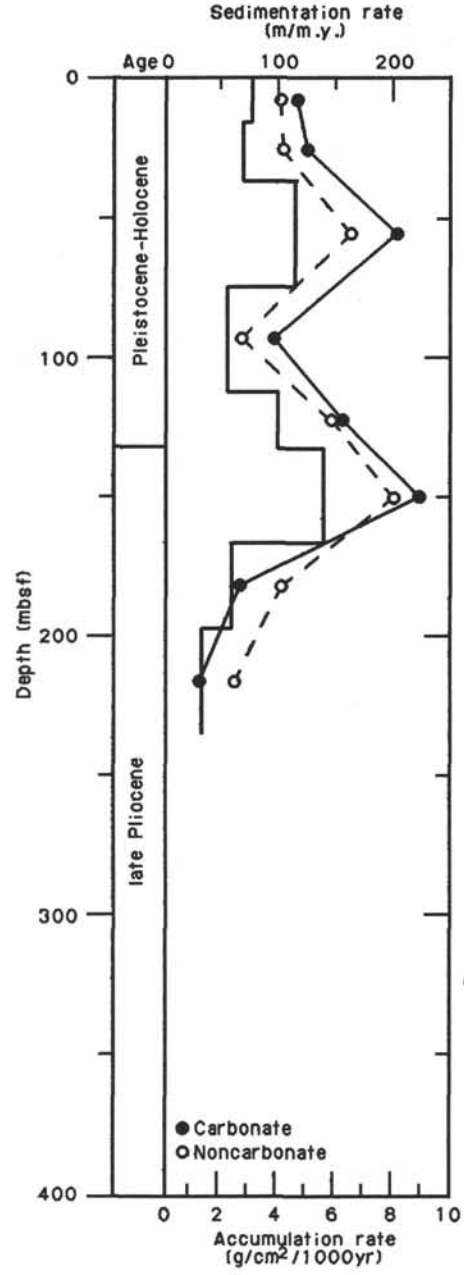

Figure 26. Sedimentation rate (solid line), calcium carbonate accumulation rate, and noncarbonate accumulation rate profiles at Site 724. Accumulation rates are plotted at the midpoint of the respective depth intervals.

Table 6. Sedimentation and accumulation rate data for Site 724.

Depth interval (mbsf)	Age range (Ma)	$CaCO_3$ ($\bar{x}$%)	C_{org} ($\bar{x}$%)	Dry-bulk density ($\bar{x}$g/cm^3)	Sed. rate ($\bar{x}$m/m.y.)	$CaCO_3$ acc. rate (g/cm^2/k.y.)	Non-$CaCO_3$ acc. rate (g/cm^2/k.y.)	C_{org} acc. rate (mg/cm^2/k.y.)
0.0–14.7	0–0.19	53.4	1.07	1.130	77.4	4.67	4.08	93.6
14.7–35.7	0.19–0.49	54.7	1.27	1.318	70.0	5.05	4.18	117.2
35.7–74.5	0.49–0.82	55.4	1.17	1.251	117.6	8.15	6.56	172.1
74.5–111.4	0.82–1.45	58.6	1.88	1.137	58.6	3.90	2.76	125.3
111.4–132.5	1.45–1.66	51.7	ND	1.214	100.5	6.31	5.89	ND
132.5–166.6	1.66–1.90	52.7	2.19	1.202	142.1	9.00	8.08	374.1
166.6–196.9	1.90–2.40	39.5	3.24	1.136	60.6	2.72	4.16	223.0
196.9–235.0	2.40–3.48	34.0	4.57	1.084	35.3	1.30	2.53	174.9

Note: ND indicates no data from the interval.

Table 7. Physical properties summary for Holes 724A, 724B, and 724C.

Core, section, interval (cm)	Depth (mbsf)	Wet-bulk density (g/cm^3)	Porosity (%)	Water content (%)	Grain density (g/cm^3)	Dry-bulk density (g/cm^3)	Vane shear strength (kPa)
117-724A-							
1H-1, 100–102	1.00	1.770	60.6	35.1	2.726	1.148	
1H-3, 90–92	3.90						10.29
1H-3, 100–102	4.00	1.690	62.3	37.8	2.646	1.051	
2H-1, 100–102	7.50	1.633	65.1	40.9	2.606	0.966	
2H-3, 100–102	10.50	1.866	49.8	27.3	2.609	1.356	12.86
2H-6, 100–102	15.00	1.932	47.5	25.2	2.664	1.446	
3H-1, 100–102	16.90	1.908	48.3	25.9	2.618	1.413	18.65
3H-3, 100–102	19.90	1.679	59.8	36.5	2.541	1.066	
3H-5, 100–102	22.90	1.824	51.1	28.7	2.546	1.300	
4H-2, 100–102	27.90	1.734	56.8	33.6	2.558	1.152	
4H-4, 100–102	30.90	1.894	52.4	28.3	2.740	1.358	41.35
4H-6, 100–102	33.90	1.960	45.8	23.9	2.673	1.491	
5H-1, 100–102	35.90	1.923	49.9	26.6	2.730	1.412	
5H-3, 100–102	38.90	1.825	54.5	30.6	2.683	1.266	30.42
5H-5, 100–102	41.90	1.800	55.4	31.6	2.648	1.232	
117-724B-							
6X-2, 70–72	47.20	1.932	52.8	28.0	2.696	1.391	
6X-4, 70–72	50.20	1.858	50.2	27.7	2.656	1.344	
7X-2, 70–72	56.90	1.741	57.5	33.9	2.587	1.152	
7X-4, 70–72	59.90	1.852	54.4	30.1	2.658	1.295	
8X-2, 80–82	66.70	1.802	53.0	30.1	2.608	1.259	
8X-4, 80–82	69.70	1.711	62.7	37.6	2.665	1.068	
9X-2, 90–92	76.40	1.643	60.7	37.8	2.582	1.022	
9X-4, 90–92	79.40	1.815	54.2	30.6	2.659	1.260	
10X-2, 90–92	86.10	1.774	57.3	33.1	2.623	1.188	
11X-2, 74–76	95.64	1.679	60.6	37.0	2.606	1.058	
11X-4, 74–76	98.64	1.774	54.8	31.6	2.633	1.213	
12X-2, 98–100	105.48	1.671	61.9	38.0	2.532	1.036	
12X-4, 68–70	108.18	1.770	56.2	32.5	2.587	1.194	
12X-6, 88–90	111.38	1.716	57.4	34.3	2.564	1.128	
14X-2, 80–82	124.70	1.773	55.2	31.9	2.561	1.207	
14X-4, 95–97	127.85	1.771	53.8	31.1	2.542	1.220	
14X-6, 90–92	130.80	1.786	55.6	31.9	2.585	1.216	
15X-2, 50–52	134.00	1.810	55.2	31.2	2.651	1.244	
16X-1, 71–73	142.41	1.751	55.9	32.7	2.561	1.178	
16X-3, 91–93	145.61	1.702	55.4	33.3	2.440	1.135	
16X-5, 77–79	148.47	1.746	56.1	32.9	2.508	1.172	
17X-2, 85–87	153.75	1.831	53.6	30.0	2.600	1.281	
17X-4, 81–83	156.71	1.786	53.6	30.7	2.537	1.237	
17X-6, 105–107	159.95	1.769	55.5	32.2	2.565	1.200	
18X-2, 50–52	163.00	1.764	55.7	32.3	2.527	1.193	
18X-4, 57–59	166.07	1.752	56.0	32.8	2.518	1.178	
19X-6, 82–84	179.02	1.725	54.3	32.3	2.471	1.168	
19X-2, 88–90	173.08	1.633	59.8	37.5	2.412	1.020	
19X-4, 74–76	175.94	1.802	52.7	29.9	2.583	1.263	
19X-6, 70–72	178.90	1.804	52.3	29.7	2.514	1.268	
20X-2, 125–127	183.15	1.821	51.4	28.9	2.553	1.295	
20X-4, 70–72	185.60	1.688	55.9	33.9	2.461	1.115	
20X-6, 75–77	188.65	1.643	60.5	37.7	2.439	1.023	
21X-3, 87–89	193.87	1.574	61.9	40.3	2.320	0.939	
22X, CC (12–14)	200.57	1.607	60.2	38.4	2.348	0.991	
23X-3, 70–72	213.10	1.484	73.4	50.7	2.484	0.731	
23X-5, 70–72	216.10	1.766	52.7	30.6	2.467	1.226	
23X-7, 20–22	218.60	1.668	58.0	35.6	2.361	1.073	
24X-2, 35–37	220.85	1.763	57.3	33.3	2.604	1.176	
24X-4, 93–95	224.43	1.702	59.4	35.8	2.504	1.094	
24X-6, 78–80	227.28	1.617	60.0	38.0	2.345	1.003	
25X-2, 47–49	230.67	1.755	56.1	32.7	2.562	1.180	
25X-4, 30–32	233.50	1.830	53.8	30.1	2.609	1.279	
25X-6, 7–9	236.27	1.815	52.6	29.7	2.627	1.276	
26X-2, 132–134	241.22	1.691	60.6	36.7	2.572	1.071	
26X-4, 4–6	242.94	1.808	50.9	28.8	2.580	1.287	
26X-6, 66–68	246.56	1.819	56.6	31.9	2.712	1.239	
27X-2, 6–8	249.56	1.764	58.4	33.9	2.678	1.165	
27X-4, 65–67	253.15	1.721	61.4	36.5	2.741	1.092	
27X-6, 7-9	255.57	1.772	56.3	32.5	2.630	1.195	
117-724C-							
1H-2, 48–50	1.98	1.678	60.3	36.8	2.595	1.060	
2H-4, 48–50	7.78	1.645	61.6	38.4	2.574	1.014	
3H-4, 48–50	17.18	1.786	58.4	33.5	2.702	1.188	

Table 7 (continued).

Core, section, interval (cm)	Depth (mbsf)	Wet-bulk density (g/cm^3)	Porosity (%)	Water content (%)	Grain density (g/cm^3)	Dry-bulk density (g/cm^3)	Vane shear strength (kPa)
117-724C-							
4H-4, 48-50	26.68	1.745	57.0	33.4	2.584	1.162	
5H-4, 48-50	36.18	1.825	53.5	30.0	2.617	1.277	
6X-4, 48-50	45.78	1.804	53.3	30.3	2.634	1.257	
7X-4, 48-50	55.48	1.744	58.7	34.5	2.664	1.143	
8X-5, 32-34	66.52	1.725	57.9	34.4	2.574	1.133	
9X-5, 50-52	76.30	1.819	56.5	31.8	2.746	1.241	
10X-4, 34-36	84.24	1.825	52.5	29.4	2.630	1.288	
11X-3, 57-59	92.57	1.807	55.8	31.7	2.645	1.235	
12X-3, 20-22	101.80	1.904	50.7	27.3	2.701	1.384	
13X-4, 87-89	113.67	1.748	57.1	33.4	2.605	1.163	
14X-5, 79-81	124.59	1.779	54.6	31.5	2.540	1.220	
15X-5, 90-92	134.30	1.848	53.5	29.7	2.672	1.300	
16X-4, 80-82	142.30	1.706	56.8	34.1	2.483	1.124	
17X-6, 67-69	154.77	1.810	55.3	31.3	2.640	1.244	
18X-5, 111-113	163.41	1.797	52.6	30.0	2.591	1.258	
19X-2, 66-68	168.06	1.770	54.3	31.4	2.563	1.214	
20X-2, 76-78	177.76	1.847	53.1	29.5	2.624	1.303	
21X-4, 59-61	190.29	1.613	60.4	38.4	2.384	0.994	
22X-3, 76-78	198.56	1.647	59.0	36.7	2.380	1.042	
22X-5, 74-76	201.54	1.679	57.4	35.0	2.454	1.091	
23X-3, 98-100	208.48	1.651	59.8	37.1	2.466	1.038	
24X-4, 76-78	219.36	1.794	54.7	31.3	2.569	1.233	
25X-4, 64-66	228.84	1.765	57.1	33.1	2.601	1.180	
26X-4, 55-57	238.45	1.799	54.1	30.8	2.618	1.245	
27X-4, 58-60	247.98	1.563	68.4	44.9	2.525	0.862	

ORGANIC GEOCHEMISTRY

Organic Matter Abundance and Character

In Holes 724A, 724B, and 724C, calcium carbonate and total carbon measurements were measured on residues of the headspace samples; the results are given in Table 3. Organic carbon values are, on average, somewhat lower than the values measured in sediments from Site 723, but they show the same trend of a general increase with depth. Several of the samples were subsequently analyzed by Rock-Eval pyrolysis, and the results are given in Table 10. The hydrogen and oxygen indices of Table 10 were recalculated using the total organic carbon (TOC) values from carbon determinations by the coulometric technique because the Rock-Eval TOC values were found to be unreliable. Plotted on a van Krevelen-type diagram (Fig. 31), the samples from Site 724 appear to be slightly shifted to the origin of the axes when compared to the sample plot from the more distal Site 723. Even though such a shift is traditionally considered to be an indication for increasing maturation, the young sediments at Site 724 are unlikely to be in a more advanced stage of thermal maturation. The temperature of maximum pyrolysis (T_{max}), which shifts to higher values during thermal maturation, is still well below the threshold of 435°C for all samples of Site 724. This is indicative for the immature organic matter expected at the site.

Hydrocarbon Gases

The results of interstitial gas analyses by the headspace method are listed in Table 11 and plotted vs. depth in Figure 32. The sharp decrease in interstitial sulfate between 25 and 50 mbsf (see "Inorganic Geochemistry" section) is closely followed by a sharp increase in methane (Fig. 32). The heavier gases, ethane and propane, show a steady increase with depth in both the headspace samples as well as in vacutainer samples from gas pockets (Figs. 32 and 33 and Tables 11 and 12). We believe that the elevated ethane and propane concentrations are of thermogenic origin for lack of a known biogenic source. Methane is dominated by biogenic production, and any elevated thermogenic methane is likely to be masked by the high biogenic contribution. Interstitial sulfate is still present at depth in low concentrations, but apparently does not inhibit methane production. Methane concentrations of 100%, as opposed to CO_2 expected during microbial sulfate reduction, were measured in gas pockets below 150 mbsf. This is in contrast to the results from Site 723, where the methane concentration of the gas pockets never reaches 100% and decreases with depth (see "Organic Geochemistry" section, "Site 723" chapter).

INTERHOLE CORRELATIONS

The upper 45 m at Site 724 has an age range from 0 to about 0.5 Ma and is characterized by cyclic changes in the nature of the sediments that can be identified by visual observation and by variations of magnetic susceptibility and carbonate content. Correlation of the sedimentary sequences and documentation of the correlative horizons between these holes provides valuable information on the relative rate of sedimentation, which is needed for any high-resolution study of Site 724 sediments.

Interhole correlations were made on the basis of visual identification of distinctive layers, as well as on the physical and magnetic properties. The magnetic susceptibility was measured at 10-cm intervals on whole-core sections.

The visual correlation of the cores relied primarily on the core photographs. Twenty-three distinct and traceable layers have been identified in the upper 80 m interval of the correlatable sedimentary sequence at Site 723 and have been labeled OM-a_1, a_2, ..., through h_4, based on the correlation between Holes 723A and 723B (see "Interhole Correlations" section, "Site 723" chapter). The letter code (e.g., a) refers to the core sequence, and the number code indicates the number of the marker layers in each core. For example, the notation "a_2" corresponds to the second marker layer defined in Core 117-723A-1H, and "b_1" denotes the first marker layer in Core 117-723A-2H. Marker layers a_1 through h_4 were defined from the cored sediments of Hole 723A. The criteria used to define a marker layer is that the layer is dis-

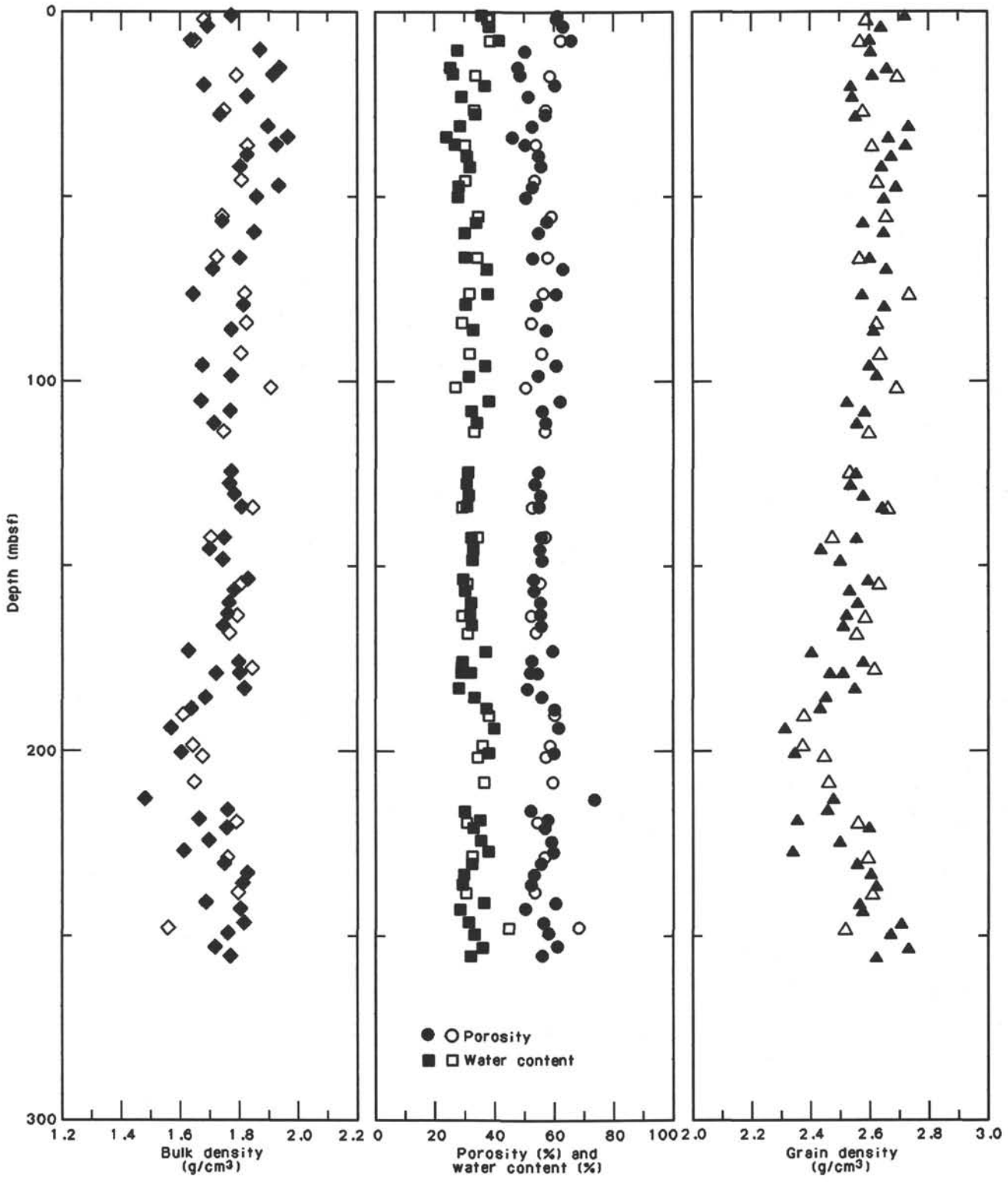

Figure 27. Index properties (wet-bulk density, porosity, water content, and grain density) measured on discrete samples from Holes 724A and 724B (solid symbols) and 724C (open symbols).

tinct enough to be traced in the sedimentary sequence of the other holes and that the character does not change. Useful criteria for recognizing the markers are color boundaries, distinctively colored layers, shape of burrow mottles, and sequence of color change in adjacent sediments. Three new marker layers were defined in the sedimentary sequence at Hole 724A, in addition to those noted at Site 723, and have been labeled c_5, e_3, and h_5, based on the correlation between the sedimentary sequences at Site 724. Table 13 lists the depths of the marker layers in the three holes of Site 724.

Figure 34 shows the magnetic susceptibility curve and positions of individual, visually correlatable layers. The pattern of

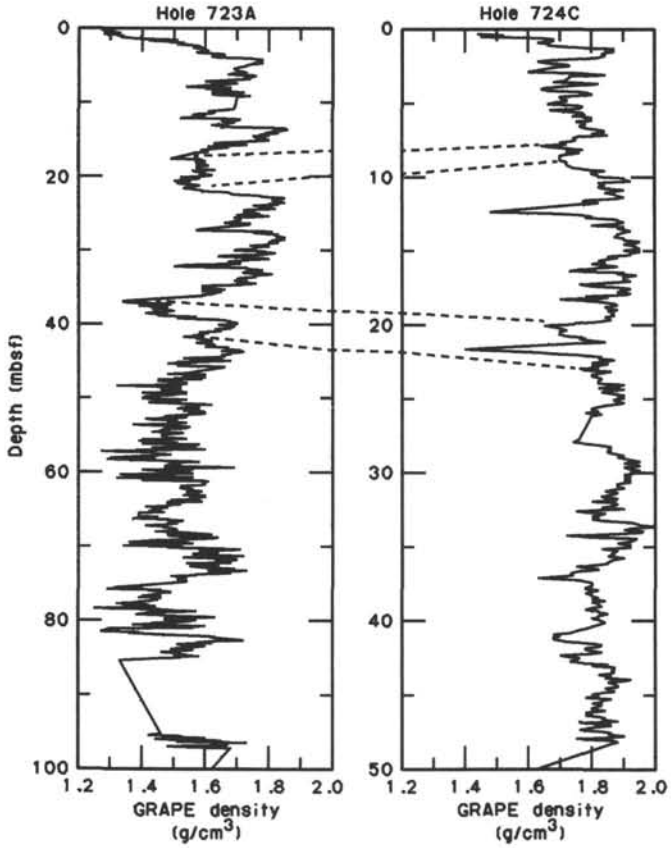

Figure 28. GRAPE wet-bulk density for Holes 723A and 724C. The profiles are based on 10-cm-thick block averages of the data. Note that the depth scale for Hole 723A is half that of Hole 724C. Tentative correlation is indicated by dashed lines.

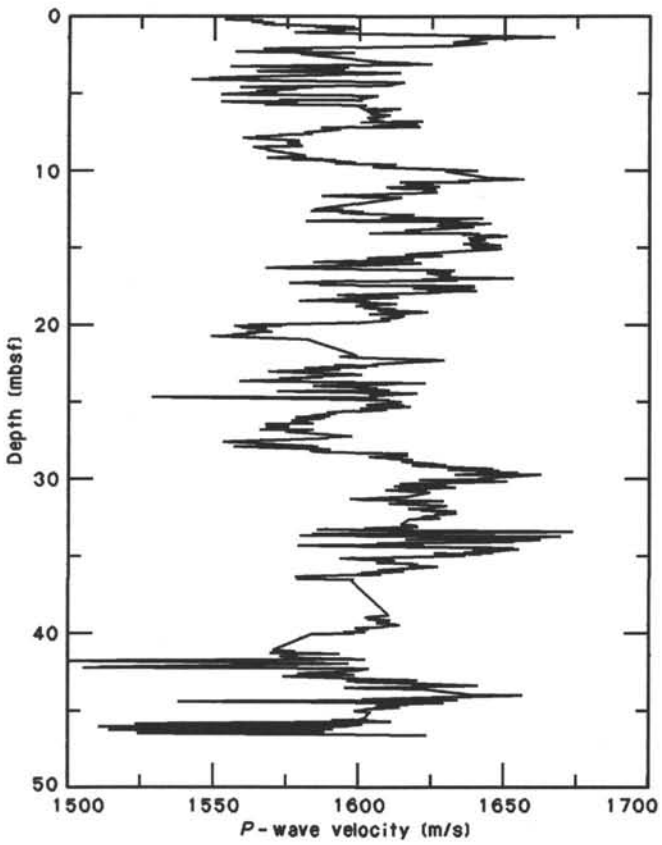

Figure 29. Compressional-wave velocity as measured by the *P*-wave logger in Hole 724C.

the susceptibility and the positions of layers match very well, not only between the three Site 724 holes but also between Sites 723 and 724 (Fig. 35). The stratigraphy of the magnetic susceptibility data and the visually identified layers is extremely consistent in that a particular visually characteristic layer always coincides in depth with a distinct feature in the magnetic susceptibility curve.

The results of the layer-by-layer correlation allow us to calculate true thickness of the layers that coincide with and are separated by core boundaries. Some core tops were expanded by water uptake during drilling. In this case, the observed apparent thickness of the disturbed sediment layer is thicker than the original thickness. In some instances, the top part of the core was missing, for which the apparent thickness is thinner than the original thickness. Fortunately, the three holes were staggered in depth, so that they have different horizons at core boundaries (Table 13). The original thickness of the layers coinciding with core tops or bottoms can be obtained by comparing thickness of the correlative layer in the continuous section of the other holes. The difference can be calculated from the differences in the ODP recorded depths of marker layers between the holes (see "A – B" and "B – C" in Table 13). Table 14 lists the differences between the depth (mbsf) calculated by the ODP Corelog data and the corrected depth (mbsf′) calculated by the layer-by-layer correlation method.

Use of the layer-by-layer method on the double- or triple-cored sedimentary sequences gives us the true stratigraphic thickness after the correction for core-boundary disturbance. Table 15 lists the stratigraphic thickness at Site 723, where most of the marker layers were defined, and Holes 724A, 724B, and 724C. The corrected depths in Holes 724A, 724B, and 724C agree well with each other. The intersite correlation of the marker layers clearly shows the differences in the rate of sedimentation.

SUMMARY AND CONCLUSIONS

Site 724 is in a water depth of about 600 m in the northern part of the ODP Leg 117 operations area on the continental margin of Oman. It is one of the central drilling targets in a depth transect bracketed by water depths ranging from 300 to 1500 m that corresponds vertically to a pronounced mid-water oxygen-minimum zone. Site 724 is positioned on the seaward flank of a slope basin that was previously drilled at Site 723, 45 km to the south. Biogenic material produced by coastal upwelling and eolian components were deposited here at a lower rate (80 m/m.y.) than in the southern part of the basin near Site 723 (175 m/m.y.). The sediments at Site 724 were expected to record changes in sedimentation and oceanographic/atmospheric circulation in considerable detail because of impeded benthic activity in the oxygen-minimum zone. Our intention in investigating Site 724 was to take advantage of the lower sedimentation rates to recover a longer Neogene section than was sampled at Site 723.

Some of the major findings at Site 724 are summarized in Figure 36 and include identification of

1. Laminated facies of late Pliocene age that are similar to, but older than, the facies found at Site 723.
2. A restricted preservation interval of abundant radiolarians and diatoms concomitant with poor preservation of plank-

Table 8. Summary of interstitial water geochemical data, Site 724.

Hole, core, section, interval (cm)	Depth (mbsf)	Vol. (mL)	pH	Alk. (mmol/L)	Sal. (g/kg)	Mg (mmol/L)	Ca (mmol/L)	Cl (mmol/L)	SO_4 (mmol/L)	PO_4 (μmol/L)	NH_4 (mmol/L)	SiO_2 (μmol/L)	Mg/Ca
724C-1H-1, 145–150	1.45	35	7.60	5.00	35.9	55.49	10.29	565	26.3	3.2	0.50	330	5.30
724A-1H-3, 145–150	4.45	35	8.10	5.40	35.0	51.24	8.59	570	19.4	3.8	1.02	512	5.98
724C-2H-4, 145–150	8.75	50	8.00	6.40	36.5	55.32	8.74	564	23.5	4.5	0.65	395	6.33
724A-3H-4, 145–150	21.85	37	7.67	5.74	35.0	45.96	9.03	572	13.9	7.3	1.35	466	5.09
724C-3H-4, 145–150	18.15	45	8.20	6.90	36.3	51.64	9.16	574	22.1	5.3	0.76	404	5.64
724C-4H-4, 145–150	27.65	45	8.20	8.68	36.2	45.38	9.78	575	13.9	3.7	1.02	483	4.64
724C-5H-4, 145–150	37.15	40	8.30	12.70	35.0	39.64	8.84	578	6.6	1.7	1.70	675	4.48
724B-6X-3, 145–150	49.45	31	—	13.02	34.0	32.35	7.47	578	0.9	2.7	2.35	963	4.33
724B-9X-4, 145–150	79.95	39	7.81	13.91	33.0	25.70	6.57	561	0.7	7.1	7.61	1148	3.91
724B-12X-5, 145–150	110.45	33	7.70	19.66	32.5	25.32	6.00	555	1.1	8.5	12.33	998	4.22
724B-16X-4, 145–150	147.65	51	7.70	21.68	32.5	23.31	4.75	557	1.8	3.5	15.04	984	4.91
724B-19X-4, 145–150	176.65	30	7.70	28.45	32.5	20.79	4.72	554	0.7	4.5	18.37	1017	4.40
724B-23X-3, 145–150	213.85	35	7.10	27.18	33.5	18.74	4.55	555	1.5	7.7	19.29	1073	4.12
724B-25X-4, 145–150	234.65	40	7.00	28.75	33.8	17.30	4.80	558	1.8	7.7	19.49	1138	3.60

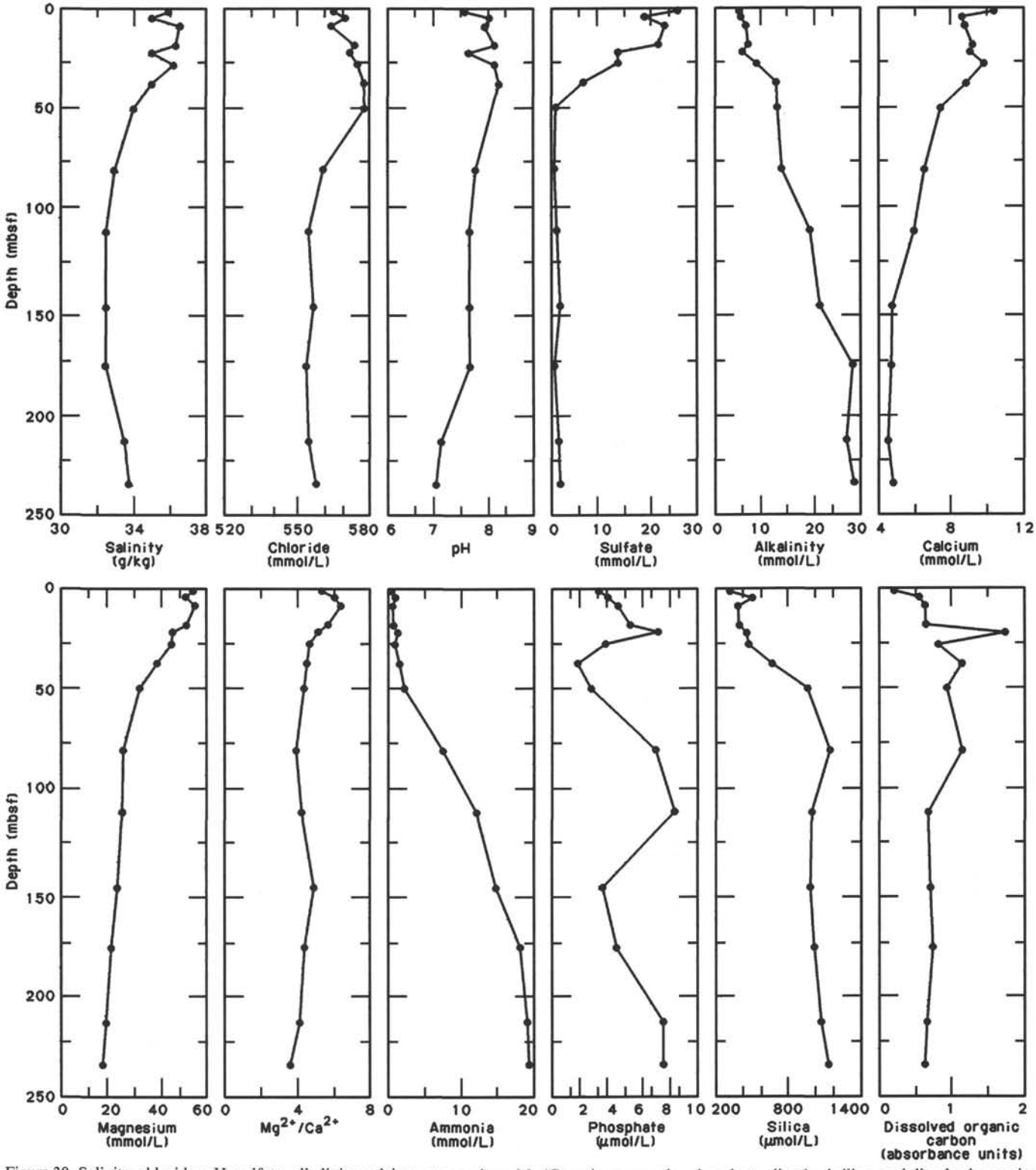

Figure 30. Salinity, chloride, pH, sulfate, alkalinity, calcium, magnesium, Mg/Ca ratio, ammonia, phosphate, dissolved silica, and dissolved organic carbon profiles for Site 724, compiled from data from three holes. Note that the data for dissolved organic carbon are plotted in terms of absorbance units and indicate relative concentration only.

tonic foraminifers. This interval occurs near the Pliocene/Pleistocene boundary and is partially coincident with the laminated facies.

3. The occurrence of shallow-water (less than 300 m) benthic foraminifers in the upper Pliocene section, which may be indicative of substantial subsidence of the site over the past 3 to 4 m.y.

4. Ongoing reduction of sulfate over the entire section and low Mg^{2+} concentrations, but a relative lack of diagenetic dolomite, in comparison to Site 723.

Table 9. Relative dissolved organic carbon concentrations at Site 724.

Core section, interval (cm)	Depth (mbsf)	Dissolved organic carbon (a.u.)
724C-1H-1, 145–150	1.45	0.209
724A-1H-3, 145–150	4.45	0.564
724C-2H-4, 145–150	8.75	0.642
724C-3H-4, 145–150	18.15	0.658
724A-3H-4, 145–150	21.85	1.740
724C-4H-4, 145–150	27.65	0.824
724C-5H-4, 145–150	37.15	1.151
724B-6X-3, 145–150	49.45	0.946
724B-9X-4, 145–150	79.95	1.156
724B-12X-5, 145–150	110.45	0.693
724B-16X-4, 145–150	147.65	0.728
724B-19X-4, 145–150	176.65	0.751
724B-23X-3, 145–150	213.85	0.673
724B-25X-4, 145–150	234.65	0.639

Note: a.u. = absorbance units at 240 nm.

5. Traces of ethane, propane, and butane that increase steadily with depth.

Only one lithologic unit was recognized at Site 724. The section ranges from uppermost lower Pliocene to the Holocene, and the magnetostratigraphy was surprisingly well defined with the Brunhes/Matuyama and Matuyama/Gauss boundaries identified at 60 and 180 mbsf, respectively (Fig. 36). The lithologic unit is comprised of green to olive green calcareous clayey silt high in organic carbon. No dolomite layers were found at this site. Interbedded in the upper Pliocene section are decimeter-scale beds of laminated diatomaceous clayey silt (Fig. 36) that are similar to, but older than, beds previously recognized at Site 723. The upper Pliocene opal-rich facies is clearly identified by the physical-property data, especially by the characteristically low grain density (Fig. 36). This facies is thought to reflect a lack of bioturbation, which led to preservation of the fine-scale laminations of heterogeneous primary input.

The faunal and floral assemblages reveal a complex environmental history at Site 724. Although indicator species generally show that monsoonal upwelling was persistent throughout the Pliocene-Pleistocene, distinct differences exist between the biotic groups (Fig. 36). Radiolarians and diatoms are abundant only in the middle upper Pliocene, an interval where planktonic foraminifers and calcareous nannofossils are rare and poorly preserved. The planktonic foraminifers become abundant and highly diverse and the calcareous nannofossils also become abundant, but with low diversity, in the uppermost Pliocene. Within this same interval, diatoms and radiolarians are sparse or absent. Hence, the production and preservation of opaline and calcareous assemblages seems to be mutually exclusive. The environmental significance of this observed abundance pattern is intriguing but unclear at this time.

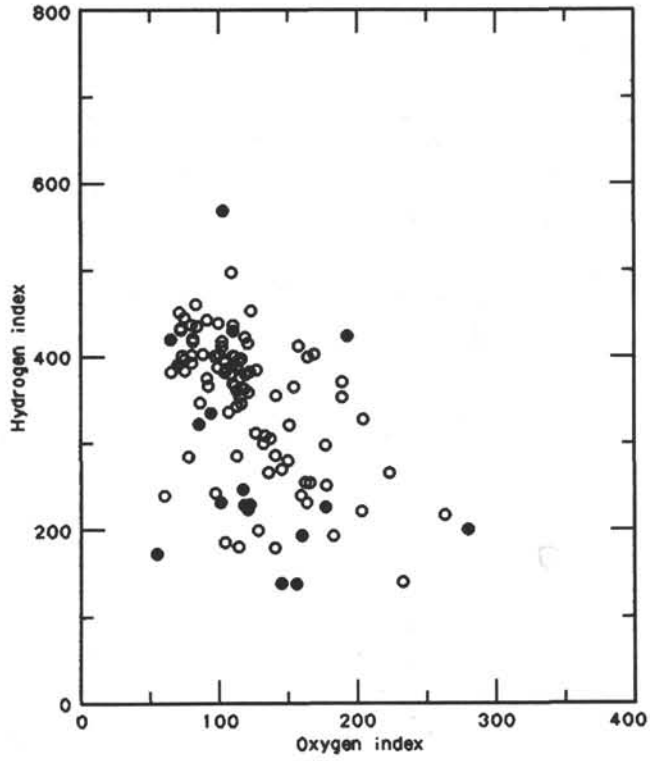

Figure 31. Plot of hydrogen index vs. oxygen index of samples from Holes 724A, 724B, and 724C (dots), compared with samples from Site 723 (circles).

Table 10. Results of Rock-Eval pyrolysis of samples from Holes 724A, 724B, and 724C.

Core, section, interval (cm)	Depth (mbsf)	T_{max} (°C)	S_1	S_2	S_3	S_2/S_3	TOC[a]	TOC[b]	HI Index	OI Index
724C-1H-2, 0–1	1.5	421	0.50	1.45	1.64	0.88	0.58	1.05	138	156
724A-1H-3, 144–145	4.44	423	0.27	1.02	1.07	0.95	0.73	0.74	138	145
724C-2H-5, 0–1	8.80	419	0.64	2.76	2.29	1.20	0.74	1.43	193	160
724A-3H-4, 144–145	21.84	423	0.51	3.48	1.65	2.10	1.33	1.41	246	117
724A-4H-2, 100–102	27.90	427	0.34	2.98	1.61	1.85	1.26	1.33	224	121
724A-4H-4, 100–102	30.90	424	0.38	2.65	2.08	1.27	1.86	1.17	226	177
724C-4H-5, 0–1	31.40	417	0.82	4.79	2.48	1.93	1.29	2.10	228	118
724A-4H-6, 100–102	33.90	423	0.10	0.64	0.90	0.71	0.73	0.32	200	280
724A-5H-1, 100–102	35.90	423	0.33	2.92	1.33	2.19	1.34	0.69	423	193
724A-5H-3, 100–102	38.90	422	0.40	3.47	1.52	2.28	1.51	1.50	231	101
724C-5H-5, 0–1	40.90	417	0.69	3.50	1.87	1.87	0.92	1.53	229	122
724A-5H-5, 100–102	41.90	415	1.06	5.97	1.53	3.90	1.85	1.39	429	110
724B-11X-4, 149–150	99.39	415	1.13	6.35	1.69	3.75	2.16	1.98	321	85
724B-12X-5, 119–120	110.19	417	0.99	6.65	1.88	3.53	2.61	1.99	334	94
724B-16X-4, 144–145	147.64	410	2.16	12.41	2.24	5.54	3.63	2.19	567	103
724B-19X-5, 0–1	176.70	407	2.85	12.64	2.27	5.56	3.94	3.24	390	70
724B-23X-4, 0–1	213.90	417	1.18	6.05	1.93	3.13	2.18	3.51	172	55
724B-25X-5, 0–1	234.70	427	0.21	8.12	1.27	6.39	3.76	1.94	419	65

Note: HI = hydrogen index and OI = oxygen index; the hydrogen and oxygen indexes were calculated on the basis of the TOC[b] values. For a detailed description of parameters, see the "Explanatory Notes" chapter (this volume).

[a] TOC values measured by Rock-Eval pyrolysis.

[b] TOC values measured by the difference method.

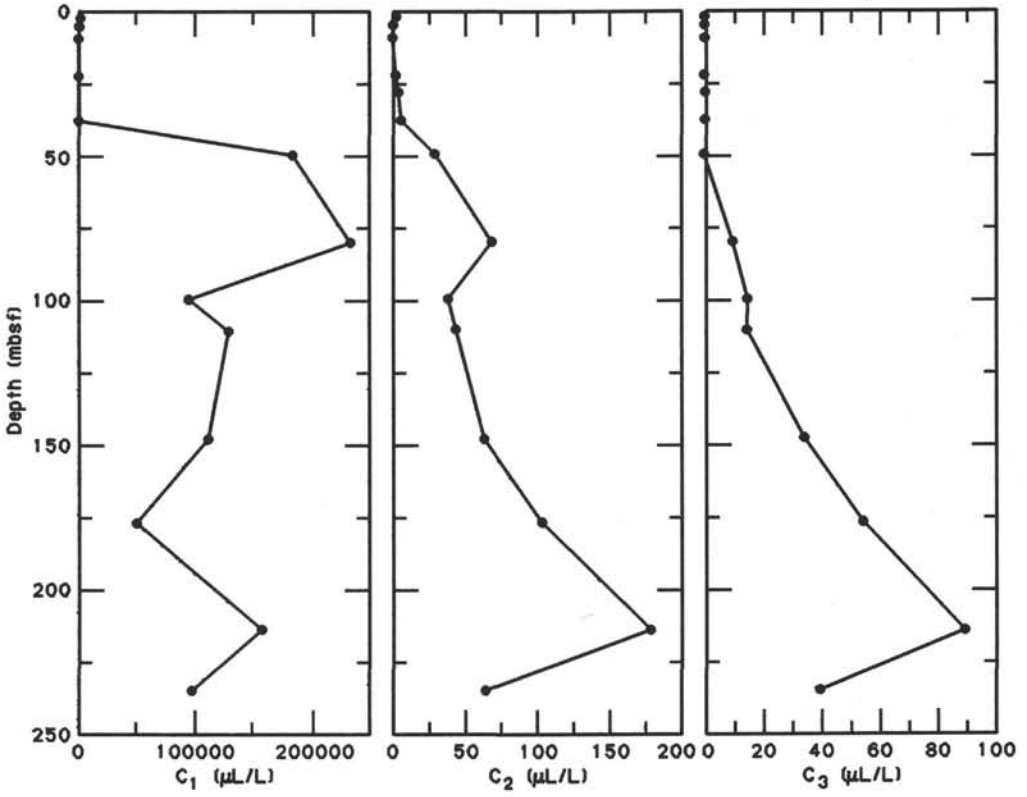

Figure 32. Downhole concentrations of methane (C_1), ethane (C_2), and propane (C_3) in headspace samples from Holes 724A, 724B, and 724C.

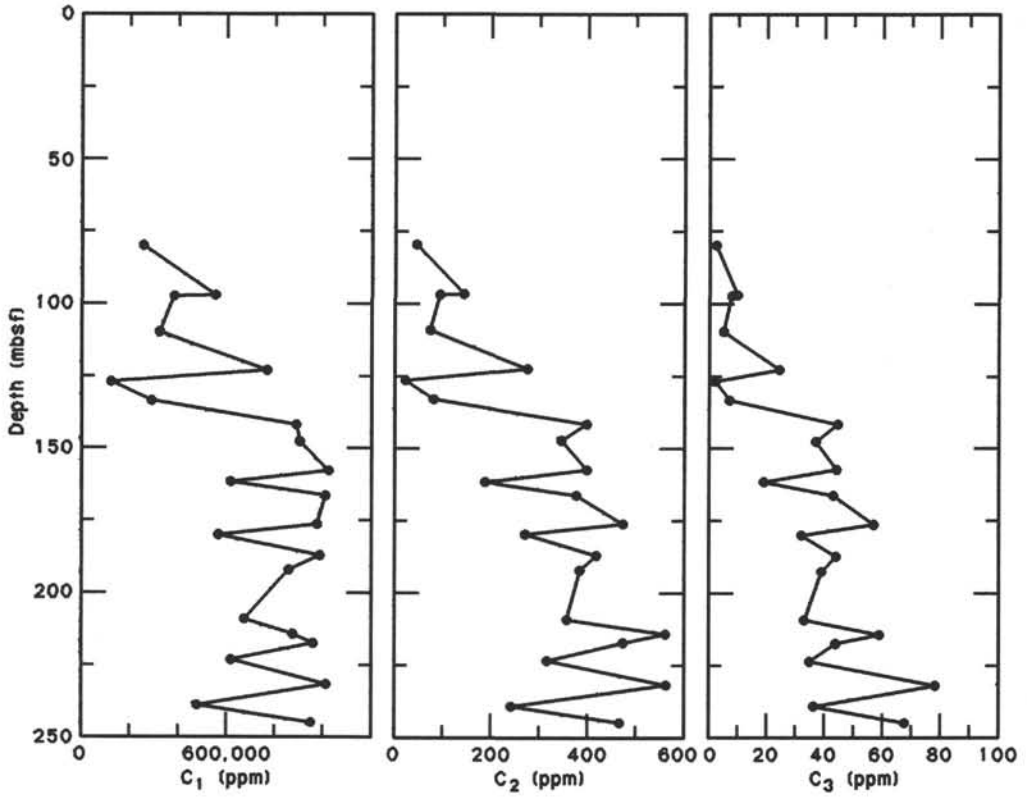

Figure 33. Downhole concentrations of methane (C_1), ethane (C_2), and propane (C_3) in vacutainer samples from gas pockets in Holes 724B and 724C.

Table 11. Concentrations of methane (C_1), ethane (C_2), and propane (C_3) per liter of wet sediment in samples from Holes 724A, 724B, and 724C.

Core, section, interval (cm)	Depth (mbsf)	C_1 (μL/L)	C_2 (μL/L)	C_3 (μL/L)	C_1/C_2
724C-1H-2, 0–1	1.50	659	2		330
724A-1H-3, 144–145	4.44	77			
724C-2H-5, 0–1	8.80	170			
724A-3H-4, 144–145	21.84	427	2		214
724C-4H-5, 0–1	27.70	111	4		28
724C-5H-5, 0–1	37.20	282	6		47
724B-6X-3, 119–120	49.19	184,525	30		6151
724B-9X-4, 119–120	79.69	235,455	70	10	3364
724B-11X-4, 149–150	99.39	95,670	40	15	2392
724B-12X-5, 119–120	110.19	130,940	45	15	2910
724B-16X-4, 144–145	147.64	113,195	65	35	1741
724B-19X-5, 0–1	176.70	51,120	105	55	487
724B-23X-4, 0–1	213.90	160,530	180	90	891
724B-25X-5, 0–1	234.70	99,720	65	40	1534

Note: Values are expressed in μL/L (volume gas/volume wet sediment).

Table 12. Concentrations of methane (C_1), ethane (C_2), and propane (C_3) measured in gas pockets from Holes 724B and 724C.

Core, section, interval (cm)	Depth (mbsf)	C_1 (ppm)	C_2 (ppm)	C_3 (ppm)	C_1/C_2
724B-9X-5, 0	80.00	263,263	50	3	5265
724B-11X-3, 68	97.08	561,013	146	10	3843
724C-11X-6, 75	97.25	392,221	99	9	3962
724B-12X-5, 40	109.40	332,980	78	6	4269
724C-14X-4, 55	122.85	775,644	278	25	2790
724B-14X-3, 145	126.85	130,426	30	3	4348
724B-15X-1, 146	133.46	300,298	89	8	3374
724C-16X-4, 44	141.94	901,650	402	45	2243
724B-16X-4, 135	147.55	915,815	348	38	2632
724B-17X-5, 20	157.60	1,031,869	402	45	2567
724C-18X-4, 95	161.75	635,001	197	20	3223
724B-18X-4, 95	166.45	1,019,407	381	44	2675
724B-19X-4, 120	176.40	985,764	476	58	2071
724C-20X-3, 145	179.95	578,441	279	33	2073
724B-20X-5, 85	187.25	998,695	422	45	2366
724B-21X-2, 78	192.28	868,933	388	40	2240
724C-23X-4, 15	209.15	683,736	361	34	1894
724B-23X-4, 50	214.40	887,847	563	60	1577
724C-24X-3, 35	217.45	967,362	478	45	2024
724B-24X-3, 147	223.47	625,838	325	36	1926
724B-25X-3, 3	231.73	1,015,347	566	79	1794
724C-26X-4, 100	238.90	486,168	251	37	1937
724B-26X-5, 30	244.70	954,141	466	68	2048

A surprising discovery is the occurrence of benthic foraminifers characteristic of shallow water (less than 300 m) in the lower upper Pliocene (Fig. 36). These data indicate that the basin may have subsided several hundred meters (as much as 600 m) during the past 3 to 4 m.y. Although seismic profiles show thickening in the center of the slope basin and thinning against the seaward basement peak, these benthic foraminifer data are the first direct indication of subsidence in the slope basins.

Carbonate and noncarbonate accumulation rates at Site 724 range from 1 to 8 g/cm²/1000 yr (Fig. 36). Superimposed on these long-term variations in sediment accumulation, both magnetic susceptibility and physical-property data show cyclic variability that may reflect shorter term, climate-related changes in the depositional system dominated by upwelling and eolian input. The production, preservation, and tectonic factors that control these changes are complex and will be the subject of post-cruise research.

Chemical compositions of interstitial waters and gas show that, unlike at Site 723, sulfate is never completely depleted at Site 724. Diagenetic effects associated with organic-matter degradation by sulfate reduction are much less obvious at Site 724. No diagenetic dolomite was encountered, the Ca/Mg ratio is much lower than at Site 723, and gas pockets contain mainly methane. Increased amounts of propane and traces of butane suggest a thermogenic origin for part of the gas.

Overall, Site 724 provides new information about the subsidence of the slope basins and on the history of carbon-rich, opal-rich laminated facies associated with the oxygen-minimum zone along the continental margin.

REFERENCES

Berggren, W. A., Kent, D. V., and Van Couvering, J. A., 1985. The Neogene: Part 2, Neogene geochronology and chronostratigraphy. *In* Snelling, N. J. (Ed.), *The Chronology of the Geological Record*: Geol. Soc. Mem. (London), 10:211–259.

Fleisher, R. L., 1974. Cenozoic planktonic Foraminifera and biostratigraphy, Arabian Sea, Deep Sea Drilling Project, Leg 23A. *In* Whitmarsh, R. B., Weser, O. E., Ross, D. A., et al., *Init. Repts. DSDP*, 23: Washington (U.S. Govt. Printing Office), 1001–1072.

Müller, P. J., and Suess, E., 1979. Productivity, sedimentation rate, and sedimentary organic matter in the oceans—I. Organic carbon preservation. *Deep-Sea Res., Part A*, 26:1347–1362.

Sato, T., Takayama, T., Kato, M., Kudo, T., and Kameo, K., in press. Calcareous microfossil biostratigraphy of the uppermost Cenozoic formations distributed in the coast of the Japan Sea. Part 4: Conclusion. *Sekiyu Gijutsu Kyokaishi*.

Takayama, T., and Sato, T., 1987. Coccolith biostratigraphy of the North Atlantic Ocean, DSDP Leg 94. *In* Ruddiman, W. F., and Kidd, R. B., Thomas, E., et al., *Init. Repts. DSDP*, 94, Pt. 2: Washington (U.S. Govt. Printing Office), 651–702.

van Morkhoven, F. P., Berggren, W. A., and Edwards, A. S., 1986. Cenozoic cosmopolitan deep-water benthic Foraminifera. *Bull. Cent. Rech. Explor.-Prod. Elf-Aquitaine*, Mem. 11.

Ms 117A-111

Table 13. Stratigraphic depths of the marker layers at Site 724.

Layer	Hole 724A Core, section, interval (cm)	Hole 724A ODP depth (mbsf)	Hole 724B Core, section, interval (cm)	Hole 724B ODP depth (mbsf)	Hole 724C Core, section, interval (cm)	Hole 724C ODP depth (mbsf)	Holes 724A – 724B	Holes 724B – 724C
OM-a_1	1H-1, 95	0.95	1H-1, 95	0.95	1H-1, 110	1.10	0.00	0.15
a_2	1H-2, 115	2.65	1H-2, 105	2.55			0.10	
b_1	1H-3, 100	4.00	1H-3, 100	4.00	2H-1, 115	3.95	0.00	−0.05
b_3	2H-1, 75	7.25	2H-1, 80	7.80	2H-4, 60	7.90	−0.55	−0.10
c_1	2H-2, 75	8.75	2H-2, 85	9.35			−0.60	
c_2	2H-3, 130	10.80	2H-3, 130	11.30	2H-6, 115	11.45	−0.50	0.15
c_3	2H-4, 70	11.70	2H-4, 75	12.25	2H-7, 50	12.30	−0.55	0.05
c_4	2H-4, 120	12.20	2H-4, 135	12.85			−0.65	
c_5	2H-5, 35	12.85	2H-5, 50	13.50	3H-1, 50	12.70	−0.65	−0.80
d_1	3H-1, 40	16.30	3H-1, 45	16.85	3H-3, 115	16.35	−0.55	−0.50
d_2	3H-1, 150	17.40	3H-2, 5	17.95	3H-4, 65	17.35	−0.55	−0.60
d_3	3H-2, 90	18.30	3H-2, 105	18.95	3H-5, 20	18.40	−0.65	−0.55
d_4	3H-3, 85	19.75	3H-3, 105	20.45	3H-6, 20	19.90	−0.70	−0.55
e_1	3H-4, 15	20.55	3H-4, 35	21.25	3H-6, 105	20.75	−0.70	−0.50
e_2	3H-5, 90	22.80	3H-5, 115	23.55	4H-1, 80	22.50	−0.75	−1.05
e_3	3H-6, 95	24.35	3H-6, 135	25.25	4H-2, 100	24.20	−0.90	−1.05
f_1	4H-1, 85	26.25	4H-1, 60	26.50	4H-4, 20	26.40	−0.25	−0.10
f_2	4H-2, 70	27.60	4H-2, 45	27.85	4H-5, 10	27.80	−0.25	−0.05
g_1	4H-4, 120	31.10	4H-4, 95	31.35	4H-7, 85	31.55	−0.25	−0.20
g_2	4H-6, 25	33.15	4H-6, 5	33.45	5H-1, 150	32.70	−0.30	−0.75
h_1	4H-7, 40	34.80	5H-1, 70	36.10	5H-3, 10	34.30	−1.30	−1.80
h_2	5H-1, 80	35.70	5H-2, 20	37.10	5H-3, 100	35.40	−1.40	−1.70
h_3	5H-2, 60	37.00	5H-2, 150	38.40	5H-4, 85	36.55	−1.40	−1.85
h_4	5H-4, 145	40.85	5H-5, 90	42.30	5H-7, 20	40.40	−1.45	−1.90
h_5	5H-5, 145	42.35	5H-6, 90	43.80	6H-1, 60	41.40	−1.45	−2.40

Note: Depths are based on ODP CORELOG data.

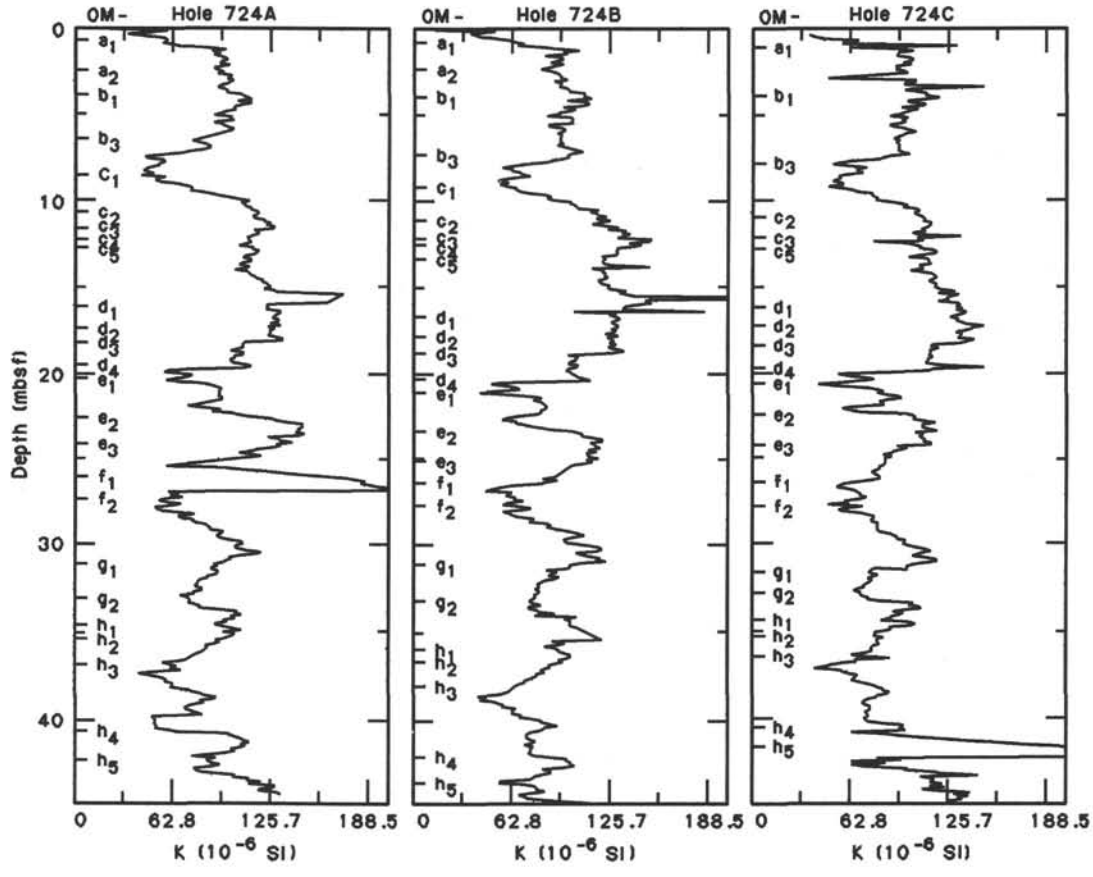

Figure 34. Volume magnetic susceptibility curves and marker layer positions in Holes 724A, 724B, and 724C.

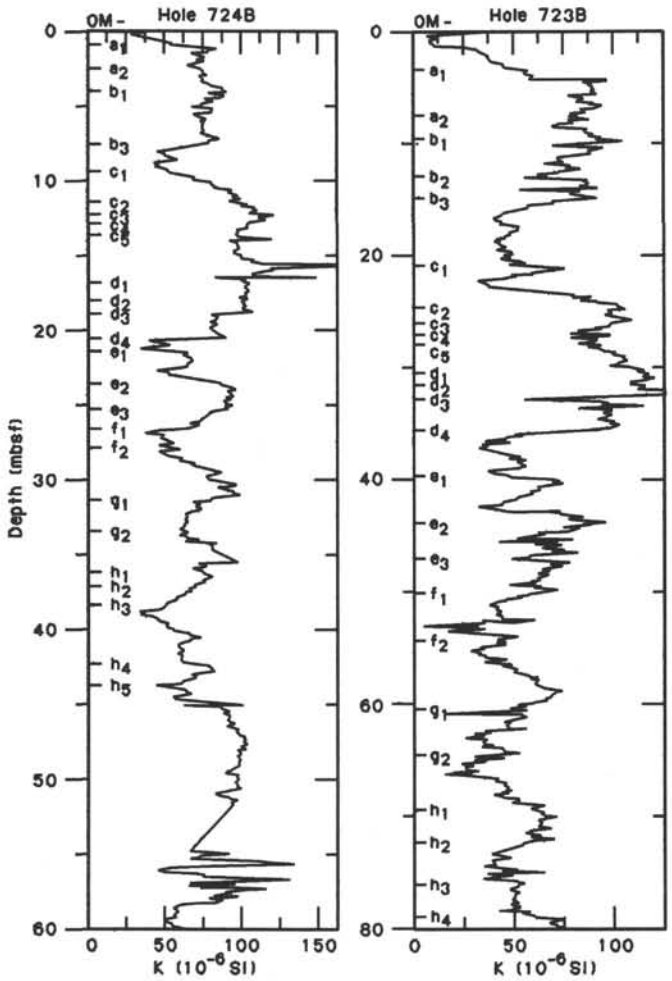

Figure 35. Volume magnetic susceptibility curves and marker layer positions in Holes 723B and 724B.

Table 14. Corrected depth below seafloor of core tops for stratigraphic calculation of depth below seafloor.

	Hole 724A			Hole 724B			Hole 724C		
Core	ODP top depth (mbsf)	Difference	Corrected top depth (mbsf)	ODP top depth (mbsf)	Difference	Corrected top depth (mbsf)	ODP top (mbsf)	Difference	Corrected top depth (mbsf)
1H	0.0	0.0	0.0	0.0	0.0	0.0	0.0	0.0	0.0
2H	6.5	0.7	7.2	7.0	0.1	7.1	2.8	0.0	2.8
3H	15.9	0.2	16.8	16.4	0.2	16.7	12.2	0.8	13.0
4H	25.4	0.6	26.9	25.9	1.0	27.2	21.7	0.5	23.0
5H	34.9	0.1	36.5	35.4	−1.1	35.6	31.2	0.7	33.2
6X							40.8	0.5	43.3

Note: ODP top depth = depth (mbsf) of core top calculated by the ODP CORELOG data; Corrected top depth = depth (mbsf) of core top calculated by the layer-by-layer correlation method. Difference is between the ODP CORELOG data depth and the depth calculated by the layer-by-layer correlation method.

Table 15. Stratigraphic depths of the marker layers at Sites 723 and 724.

	Hole 723B		Hole 724A		Hole 724B		Hole 724C	
Layer	Core, section, interval (cm)	Corrected depth (mbsf)	Core, section, interval (cm)	Corrected depth (mbsf)	Core, section, interval (cm)	Corrected depth (mbsf)	Core, section, interval (cm)	Corrected depth (mbsf)
OM-a_1	1H-3, 35	3.35	1H-1, 95	0.95	1H-1, 95	0.95	1H-1, 110	1.10
a_2	2H-3, 20	7.20	1H-2, 115	2.65	1H-2, 105	2.55		
b_1	2H-4, 65	9.15	1H-3, 100	4.00	1H-3, 100	4.00	2H-1, 115	3.95
b_2	2H-6, 110	12.60						
b_3	3H-1, 95	14.75	2H-1, 75	7.95	2H-1, 80	7.90	2H-4, 60	7.90
c_1	3H-5, 110	20.90	2H-2, 75	9.45	2H-2, 85	9.45		
c_2	4H-1, 85	24.95	2H-3, 130	11.50	2H-3, 130	11.40	2H-6, 115	11.45
c_3	4H-2, 100	26.60	2H-4, 70	12.40	2H-4, 75	12.35	2H-7, 50	12.30
c_4	4H-3, 15	27.25	2H-4, 120	12.90	2H-4, 135	12.95		
c_5	4H-3, 100	28.10	2H-5, 35	13.55	2H-5, 50	13.60	3H-1, 50	13.50
d_1	4H-5, 70	30.80	3H-1, 40	17.20	3H-1, 45	17.15	3H-3, 115	17.15
d_2	4H-6, 10	31.70	3H-1, 150	18.30	3H-2, 5	18.25	3H-4, 65	18.15
d_3	4H-7, 5	33.15	3H-2, 90	19.20	3H-2, 105	19.25	3H-5, 20	19.20
d_4	5H-2, 50	35.30	3H-3, 85	20.65	3H-3, 105	20.75	3H-6, 20	20.70
e_1	5H-5, 20	39.50	3H-4, 15	21.45	3H-4, 35	21.55	3H-6, 105	21.55
e_2	6H-1, 90	43.80	3H-5, 90	23.70	3H-5, 115	23.85	4H-1, 80	23.80
e_3	6H-3, 150	47.40	3H-6, 95	25.25	3H-6, 135	25.55	4H-2, 100	25.50
f_1	6H-5, 120	50.10	4H-1, 85	27.75	4H-1, 60	27.80	4H-4, 20	27.70
f_2	7H-2, 15	54.25	4H-2, 70	29.10	4H-2, 45	29.15	4H-5, 10	29.10
g_1	7H-6, 30	60.40	4H-4, 120	32.60	4H-4, 95	32.65	4H-7, 85	32.85
g_2	8H-2, 60	64.40	4H-6, 25	34.65	4H-6, 5	34.75	5H-1, 150	34.70
h_1	8H-5, 90	69.20	4H-7, 40	36.30	5H-1, 70	36.30	5H-3, 10	36.30
h_2	9H-1, 20	72.10	5H-1, 80	37.30	5H-2, 20	37.30	5H-3, 100	37.20
h_3	9H-3, 135	76.25	5H-2, 60	38.60	5H-2, 150	38.60	5H-4, 85	38.55
h_4	9H-7, 95	81.85	5H-4, 145	42.45	5H-5, 90	42.50	5H-7, 20	42.40
[a]h_5			5H-5, 145	43.95	5H-6, 90	44.00	6X-1, 60	43.90

Note: Depths are based on the correction factor of Table 14. Corrrected depth = corrected depth for stratigraphic thickness.
[a] Top of bioturbated white layer overlain by dark layer.

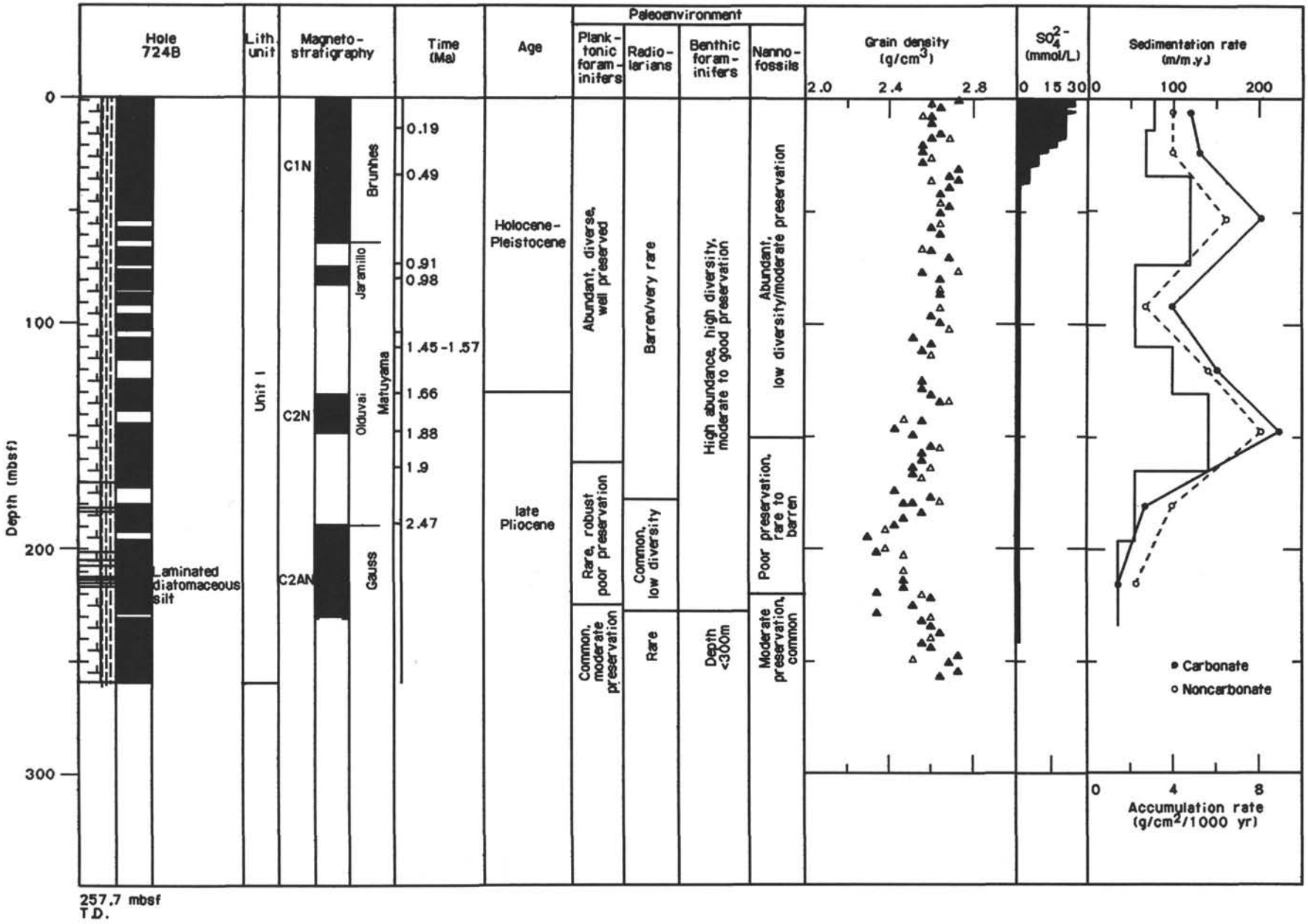

Figure 36. Summary of preliminary shipboard analyses at Site 724.